Mycosphere

ARTICLE

Open Access

https://doi.org/10.48130/mycosphere-0026-0005

Mycosphere **2026**, 17: e004

Global phylogeny, divergence times and evolutionary history of *Trichaptum* s.l. (Hymenochaetales, Basidiomycota): two new families and six new species

Meng Zhou[1,2#], Yujin Cui[1#], Josef Vlasák[3], Yingda Wu[4], Chenxi Li[2], Guangyu Zeng[5], Lei Zhuang[6] and Yuan Yuan[1*]

[1] *School of Ecology and Nature Conservation, Beijing Forestry University, Beijing 100083, China*
[2] *State Key Laboratory of Efficient Production of Forest Resources & MOE Key Laboratory of Wooden Material Science and Application, Beijing Forestry University, Beijing 100083, China*
[3] *Biology Centre of the Academy of Sciences of the Czech Republic, České Budějovice 31, CZ-370 05, Czech Republic*
[4] *Key Laboratory of Forest and Grassland Fire Risk Prevention, Ministry of Emergency Management, China Fire and Rescue Institute, Beijing 102202 China*
[5] *Guangxi Forestry Science Research Institute, Nanning 530002, China*
[6] *Harbin Academy of Agricultural Sciences, Harbin 150028, China*
[#] Authors contributed equally: Meng Zhou, Yujin Cui
[*] Correspondence: yuanyuan1018@bjfu.edu.cn (Yuan Y)

Abstract

The species diversity of *Trichaptum* s.l., a significant group within the polypore fungi, has expanded substantially in recent years. However, its higher-level taxonomy and evolutionary origins remain underexplored. In this study, the evolutionary history of *Trichaptum* s.l. is presented using phylogenetic, morphological, and molecular-clock analyses. The results resolve *Trichaptum* s.l. into four families: Hirschioporaceae, Trichaptaceae, and two newly proposed families, Podocarpioporaceae fam. nov. and Pseudotrichaptaceae fam. nov. Consequently, the *Trichaptum* complex s.l. now comprises seven genera (*Hirschioporus*, *Nigrohirschioporus*, *Pallidohirschioporus*, *Perennihirschioporus*, *Pseudotrichaptum*, *Podocarpioporus*, and *Trichaptum* s.s.), and 55 taxa. The six new species from the tropical and subtropical regions are described: *Nigrohirschioporus keylargoensis* sp. nov., *Nigrohirschioporus wuyiensis* sp. nov., *Perennihirschioporus caymanensis* sp. nov., *Podocarpioporus hydnoides* sp. nov., *Trichaptum cystidiolatum* sp. nov., and *Trichaptum longisporum* sp. nov. Molecular clock dating analysis suggests that familial divergence within *Trichaptum* s.l. occurred during the Cretaceous period (71–119 Mya). Ancestral state reconstruction analysis indicates a complex evolutionary history, potentially originating in Central and East Asia. However, the origins of the four families show notable differences, with two major origin groups in Asia and the Americas. Ecological niche modeling (Maxent) reveals that *Trichaptum* s.l. likely originated in tropical regions and subsequently expanded into subtropical, temperate, and montane zones, a transition accompanied by the evolution of harder basidiomata. Climatic factors, such as the maximum temperature of the warmest month (Bio5), were identified as primary drivers of the distribution of *Hirschioporus*, *Pallidohirschioporus*, and *Pseudotrichaptum*. The precipitation of the wettest quarter (Bio16) was the dominant factor driving the distribution of *Perennihirschioporus*. The mean temperature of the coldest quarter (Bio11) was the primary limiting factor for *Nigrohirschioporus*. The minimum temperature of the coldest month (Bio6), and the annual precipitation (Bio12) showed the highest percentage contribution to the distribution of *Trichaptum* s.s. This study provides a robust framework for understanding the systematics, evolution, and biogeography of *Trichaptum* s.l.

Citation: Zhou M, Cui Y, Vlasák J, Wu Y, Li C, et al. 2026. Global phylogeny, divergence times and evolutionary history of *Trichaptum* s.l. (Hymenochaetales, Basidiomycota): two new families and six new species. *Mycosphere* 17: e004 https://doi.org/10.48130/mycosphere-0026-0005

Introduction

Despite rapid growth in documented fungal diversity—with over 160,000 species known (https://nmdc.cn/fungalnames, accessed on March 6, 2025) and thousands added annually[1–4]—known species represent only a fraction of estimates, keeping species discovery and evolutionary reconstruction key priorities in mycology[5–8]. The origin and evolution of organisms are among the most important issues in life sciences, while molecular-clock analyses and biogeographic studies aim to reconstruct the origin, speciation, and distribution patterns[9–11]. While molecular clock and biogeographic analyses help reconstruct these evolutionary contexts, fungal studies still lag behind animals and plants due to challenges like cryptic morphology, insufficient sampling, and scarce fossil records[12–16]. Fortunately, significant progress has been made in the study of macrofungi such as the Agaricomycetes, Hymenochaetales, and Boletaceae[17–21].

Wood-inhabiting fungi, as an important group of macrofungi, have rich species diversity, nutritional types, morphological variety, and are widely distributed in forest ecosystems. They play multiple roles, such as saprotrophy, parasitism, and symbiosis, with significant ecological and economic values[22–31]. In recent years, a series of studies have addressed the species diversity and evolutionary history of wood-inhabiting fungi[32–35], including the genus *Trichaptum* s.l.[36–40].

The genus *Trichaptum* s.l., typified by *Trichaptum perrottetii* (Lév.) Ryvarden (basionym: *Polyporus trichomallus* Berk. & Mont.), was established by Murrill in 1904[41]. It is characterized by annual to perennial, mostly pileate basidiomata with a hispid to adpressed tomentose abhymenial surface, variable hymenophore (irpicoid, lamellate, or poroid), with brownish to purplish hymenial surface, duplex context, mainly a dimitic hyphal system with clamped generative hyphae, predominantly cylindrical basidiospores, and the presence of cystidia[39,42,43]. *Trichaptum* s.l. species are widely distributed in forest ecosystems, functioning as dominant white-rot decomposers. Ecological surveys have highlighted their prevalence in deadwood communities; for instance, *Trichaptum abietinum* was identified as the most frequent species in recent field studies, recording 145 fruit-body occurrences across 571 sampled logs, significantly outperforming other wood-inhabiting fungi[44,45].

Beyond their ecological dominance, these species possess considerable economic and biotechnological potential. While traditionally noted for the medicinal values of species such as *T. abietinum, T. biforme*, and *T. byssogenum*[46,47], recent research has expanded their utility into sustainable materials. *Trichaptum biforme* has been successfully evaluated as a novel mycelium source for fabricating bio-foams, offering a competitive, biodegradable alternative to commercial plastic packaging[48]. Currently, *Trichaptum* s.l. is divided into two families, seven genera, and 49 species based on morphological characters, phylogenic analyses, and divergence times estimation[39].

The family Hirschioporaceae includes four genera: *Hirschioporus*, *Nigrohirschioporus*, *Pallidohirschioporus*, and *Perennihirschioporus*. The family Trichaptaceae consists of a single genus, *Trichaptum*, while two other genera, *Pseudotrichaptum* and *Podocarpioporus*, are treated as incertae sedis within the order Hymeonchaetales[39]. Resolving their phylogenetic relationship and taxonomic status is of importance for future development and utilization of resources. Furthermore, with the increase in collection sites and samples, the number of new species will continue to grow. Although Zhou et al. conducted a preliminary study on the origin and divergence time of *Trichaptum* s.l.[39], an in-depth study of this group is urgently needed.

Determining the spatial-distribution ability of species is crucial for understanding the environmental factors influencing them and their biodiversity. Niche modeling is a useful tool for assessing the potential geographic distribution of species and has been widely applied in the fields of biogeography, ecology, and evolutionary phylogenetics[49–51]. Many statistical models are available to simulate species distribution types and the diversity of species' spatial patterns[52–54]. The Maximum Entropy (Maxent) model is widely used to predict the potential distribution of species based on collection data and environmental information, with some advantages, including strong performance even when data are incomplete, user-friendliness, the ability to perform well with limited occurrence data, and high simulation accuracy[55–57]. Previous studies have conducted habitat suitability predictions and explored the impact of environmental factors on the distribution of fungal groups[58–60], however, *Trichaptum* s.l. has not yet been carried out.

In this study, we used newly collected specimens to update the classification system, and reconstruct the evolutionary history of *Trichaptum* s.l., combined with multi-gene phylogenetic analyses, morphological characteristics, and molecular-clock analyses. Based on this revised taxonomic framework, a global occurrence dataset was compiled for each genus. Ecological niche modeling (Maxent) was employed to quantify the climatic niche of each lineage and to identify the key environmental drivers of their respective geographical distributions, providing a clearer understanding of their unique adaptive strategies.

Materials and methods

Specimen collection

In this study, 28 new specimens of *Trichaptum* s.l. were collected from eight countries, including China, Brazil, Bolivia, Costa Rica, Ecuador, French Guiana, Jamaica, and the USA. All the studied specimens were deposited in the Fungarium of the Institute of Microbiology, Beijing Forestry University (BJFC, China), and the private herbarium of Josef Vlasák (JV, Czech Republic).

Morphological studies

Macromorphological descriptions are based on field collection records and voucher observations of basidiomata. The micromorphological data were obtained by dissecting dried specimens and observing them under a stereomicroscope (Nikon E80i microscope, Tokyo, Japan), following previous studies[39,61], and line drawings were made with the aid of a drawing tube. Special color terminology used follows Anonymous[62] and Petersen[63]. Specimen sections were prepared and mounted in Melzer's reagent, Cotton Blue, and 5% KOH.

The following abbreviations are used: KOH = 5% potassium hydroxide; CB = Cotton Blue; CB+ = cyanophilous in Cotton Blue; CB– = cyanophilous in Cotton Blue; IKI = Melzer's reagent; IKI– = neither amyloid nor dextrinoid in Melzer's reagent; L = mean basidiospore length (arithmetic average of basidiospores); W = mean basidiospore width (arithmetic average of basidiospores); Q = variation in the L/W ratios between specimens studied; n (a/b) = number of basidiospores (a) measured from the given number of specimens (b), 'n' presenting basidiospore size variation, 5% of measurements were excluded from each end of the range and these values are given in parentheses. The texture was evaluated using the following scale: Grade I (Soft corky), tissue is soft, compressible, and easily deformed; Grade II (Coriaceous), tissue is tough, leather-like, and pliable; Grade III (Hard corky), tissue is firm, resists deformation, but retains some elasticity; and Grade IV (Woody), tissue is rigid, non-deformable, and highly lignified.

DNA extraction, polymerase chain reaction, and sequencing

Total DNA was extracted from the dried specimens using the standard protocol of the rapid plant genome extraction kit-DN14 (Aidlab Biotechnologies Co., Ltd, Beijing, China), with modifications based on a previous study by Zhou et al.[39]. Five gene fragments, including internal transcribed spacer (ITS), nuclear large subunit rDNA (nLSU), translation elongation factor 1 (TEF1), mitochondrial small subunit rDNA (mt-SSU), and nuclear small subunit rDNA (nuc-SSU), were amplified using polymerase chain reaction (PCR) to obtain target products. The selected target fragments and their primer sequences are listed in Table 1. Amplification was performed in a 30 μL reaction system (2× EasyTaq® PCR SuperMix: ultra pure water : forward primer : reverse primer : template DNA = 15:12:1:1:1). PCRs were carried out using S1000™ Thermal Cycler (Bio-Rad Laboratories, California, USA), following the procedure by Zhou et al.[39]. The PCR products were sequenced on the ABI-3730-XL DNA analyzer (Applied Biosystems, Foster City, CA, USA) by Beijing Genomics Institute (Beijing, China) with the sample primers in Table 1. Finally, all the newly generated sequences were deposited in the NCBI GenBank database, and the accession numbers are listed in Table 2.

Datasets

In this study, three datasets were used for the phylogenetic analyses, divergence time estimation, as well as the historical biogeography and ancestral state of the basidiomata. Dataset 1 included five gene fragments, namely ITS, nLSU, TEF1, mt-SSU, and nuc-SSU, from 157 specimens, for the phylogenetic analyses (Table 2). Dataset 2 consisted of three gene fragments, including ITS, nLSU, and TEF1, from 124 specimens, to estimate the divergence time of *Trichaptum* s.l. (Table 2 and Supplementary Table S1). Dataset 3 also contained three gene fragments, including ITS, nLSU, and TEF1, from 52

Table 1. Primer information for five gene fragments in this study.

Sequence	Primers	Primers sequence (5'–3')	Ref.
ITS	ITS4	TCC TCC GCT TAT TGA TAT GC	[64]
	ITS5	GGA AGT AAA AGT CGT AAC AAG G	
nLSU	LR0R	ACC CGC TGA ACT TAA GC	[65]
	LR7	TAC TAC CAC CAA GAT CT	
mt-SSU	MS1	CAG CAG TCA AGA ATA TTA GTC AAT G	[64]
	MS2	GCG GAT TAT CGA ATT AAA TAA C	
TEF1	983F	GCY CCY GGH CAY CGT GAY TTY AT	[66]
	1567R	ACH GTR CCR ATA CCA CCR ATC TT	
nuc-SSU	NS1	GTA GTC ATA TGC TTG TCT C	[64]
	NS4	CTT CCG TCA ATT CCT TTA AG	

specimens, to infer the historical biogeography and ancestral state of the basidiomata (Table 2 and Supplementary Table S1).

Phylogenetic analyses

All the sequences of the five gene fragments were aligned separately using MAFFT v. 7.0[67], manual editing and adjustments of bases were performed in BioEdit v. 7.0.9[68], and then combined with the five gene fragments as a dataset. The best optimal model for the combined dataset was determined using ModelTest-NG v0.1.7[69]. Phylogenetic analyses were performed using Maximum Likelihood (ML) and Bayesian Inference (BI) using RAxML v. 8.2.12[70] and MrBayes v. 3.2.6[71], respectively. For ML analysis, bootstrap support values (BS) were estimated with 1,000 replicates using default parameters. For BI analysis, Bayesian posterior probabilities (BPP) were calculated with two million generations, and the first 25% were discarded as burn-in. Finally, the ML and BI trees were visualized using Figtree v1.4.4 (https://tree.bio.ed.ac.uk/software/figtree). Nodes with ML bootstrap values below 50% and BI posterior probabilities below 0.90 were excluded from consideration.

Divergence time estimation of *Trichaptum* s.l.

The divergence time estimation of *Trichaptum* s.l. was based on three gene fragments (ITS, nLSU, and TEF1) from 124 specimens, following the methods of previous studies[18,33,39]. Briefly, XML was generated using BEAUTi v. 2.6.6[72] with the most optimal model of the GTR substitution model, which was estimated by ModelTest-NG v0.1.7[69], using a log-normal relaxed molecular clock and Yule speciation prior. Three fossil calibration points with established fossil records were selected: 1) 90 Mya representing the minimum age of Agaricales[73,74]; 2) 125 Mya representing the minimum age of Hymenochaetaceae[75,76]; and 3) 400 Mya representing the divergence time between the Ascomycota and the Basidiomycota[77,78]. The offset age with a gamma-distributed prior (scale = 20 and shape = 1) was set as 90, 125, and 400 Mya for Agaricales, Hymenochaetaceae, and Basidiomycota, respectively. Four independent Markov Chain Monte Carlo (MCMC) chains were run for 100 million generations, with tree sampling every 1,000 generations. Tracer v. 1.5 (https://beast.bio.ed.ac.uk/Tracer) was used to check the results log file to confirm that ESS ≥ 200. FigTree v. 1.4.4 (https://tree.bio.ed.ac.uk/software/figtree) was used to summarize the Maximum Clade Credibility (MCC) tree with 95% Highest Posterior Density (HPD) intervals, removing 20% as burn-in and setting the posterior probability limit to 0.80.

Inferring historical biogeography and ancestral state of basidiomata

The historical biogeography and ancestral state of basidiomata of *Trichaptum* s.l. were inferred using Reconstruct Ancestral State in Phylogenies v. 4.2 (RASP)[79,80] under the Statistical Dispersal-Extinction-Cladogenesis (S-DEC) model and the Bayesian Binary MCMC model. The distribution of *Trichaptum* s.l. species was divided into six geographic zones, viz., A) Central and South America, B) North America, C) Europe, D) Central and East Asia, E) South to Southeast Asia and Oceania, and F) Africa, as well as four climate zones, namely A) temperate zones, B) subtropical zones, C) tropical zones, and D) mountain zones. The consistency and pileal surface morphology of basidiomata were classified into four and five types, respectively. The four types of consistency were A) Soft corky, B) Coriaceous, C) Hard corky, and D) Woody. The five types of pileal surface were A) Tomentose, B) Smooth, C) Warted, D) Hispid, and E) Apileate.

Species distribution and environmental factors

Records of *Trichaptum* s.l. were gathered from global field survey sites and the online database of the Global Biodiversity Information Facility (GBIF, www.gbif.org, accessed on 1st Oct, 2025), prioritizing samples with molecular or photographic verification. For records lacking precise geo-coordinates, Google Maps (www.google.com/maps) was used to estimate approximate latitude and longitude based on the described geographic locations. The dataset underwent rigorous cleaning. First, duplicate distribution points were filtered based on longitude and latitude coordinates. To mitigate

Table 2. Taxa information and GenBank accession numbers used in this study.

Family	Species	Voucher	Locality	GenBank A accession no.					Ref.
				ITS	nLSU	mt-SSU	TEF1	nuc-SSU	
Coltriciaceae	*Coltricia perennis*	Cui 10319	China	KU360687	KU360653	—	KY693935	—	[104]
Coltriciaceae	*Coltricia dependens*	Dai 10944	China	KY693737	KY693757	—	—	—	Genbank
Neoantrodiellaceae	*Neoantrodiella gypsea*	Cui 10372	China	KT203290	MT319396	MT326567	—	—	[105]
Neoantrodiellaceae	*Neoantrodiella gypsea*	Yuan 5589	China	KT203292	KT203313	—	—	—	Genbank
Neoantrodiellaceae	*Neoantrodiella thujae*	Dai 5065	China	KT203293	MT319397	MT326568	—	—	[105]
Nigrofomitaceae	*Nigrofomes melanoporus*	JV 1704/39	Costa Rica	MF629835	MF629831	—	—	—	[106]
Nigrofomitaceae	*Nigrofomes melanoporus*	JV 1607/82	Costa Rica	MF381027	—	—	—	—	[36]
Nigrofomitaceae	*Nigrofomes sinomelanoporus*	Cui 5277	China	MF629836	MT319398	—	—	—	[105–106]
Nigrofomitaceae	*Nigrofomes sinomelanoporus*	Dai 16286	China	MF629839	—	—	—	—	[106]
Hirschioporaceae	*Hirschioporus abietinus*	Cui 2667	China	OQ449096	OQ449033	—	OQ831431	OQ449408	[39]
Hirschioporaceae	*Hirschioporus abietinus*	CBS 221.53	France	MH857167	MH868703	—	—	—	[107]
Hirschioporaceae	*Hirschioporus abietinus*	Dai 1	Finland	OQ449044	—	—	—	—	[39]
Hirschioporaceae	*Hirschioporus abietinus*	Dai 12337	China	OL504712	OL477386	OQ517075	OQ831434	OQ449409	[39]

(to be continued)

Table 2. (continued)

Family	Species	Voucher	Locality	GenBank A accession no.					Ref.
				ITS	nLSU	mt-SSU	TEF1	nuc-SSU	
Hirschioporaceae	*Hirschioporus abietinus*	Dai 23792	China	OQ449043	OQ449038	OQ517079	—	OQ448998	[39]
Hirschioporaceae	*Hirschioporus abietinus*	KUC20130719-05	Korea	KJ668437	KJ668289	—	—	—	[108]
Hirschioporaceae	*Hirschioporus abietinus*	FSU 2734	Germany	EU484271	—	—	—	—	[109]
Hirschioporaceae	*Hirschioporus abietinus*	JV 0907/9	Czechia	MF381023	—	—	—	—	[36]
Hirschioporaceae	*"Hirschioporus abietinus"*	BFOTU23	Finland	AM901859	—	—	—	—	[110]
Hirschioporaceae	*"Hirschioporus abietinus"*	Cui 9627	China	OQ449046	OQ449184	OQ517080	—	OQ448999	[39]
Hirschioporaceae	*"Hirschioporus abietinus"*	Dai 18909	China	OQ449048	OQ449185	OQ449111	OQ831436	OQ449001	[39]
Hirschioporaceae	*"Hirschioporus abietinus"*	Dai 23763	China	OQ449131	OQ449195	OQ449116	—	OQ449006	[39]
Hirschioporaceae	*Hirschioporus acontextus*	Cui 11830	China	OQ449138	OQ449198	OQ449120	—	OQ449010	[39]
Hirschioporaceae	*Hirschioporus acontextus*	Dai 19097	China	OQ449140	OQ449199	OQ449122	—	OQ449012	[39]
Hirschioporaceae	*Hirschioporus acontextus*	Dai 23793	China	OQ449141	OQ449200	OQ449123	OQ831439	OQ449013	[39]
Hirschioporaceae	*Hirschioporus acontextus*	KUC20131001-03	Korea	KJ668436	KJ668288	—	—	—	[39]
Hirschioporaceae	*Hirschioporus beijingensis*	Dai 18907	China	OQ449142	OQ449201	OQ449124	OQ831440	OQ449014	[39]
Hirschioporaceae	*Hirschioporus beijingensis*	Dai 23704	China	OQ449143	OQ449202	OQ449125	OQ831441	OQ449015	[39]
Hirschioporaceae	*Hirschioporus chinensis*	Cui 2488	China	OQ449146	—	OQ449126	OQ831442	OQ449016	[39]
Hirschioporaceae	*Hirschioporus chinensis*	Dai 19110	China	OQ449098	—	—	—	—	[39]
Hirschioporaceae	*Hirschioporus chinensis*	Dai 19111	China	OQ449099	—	—	—	—	[39]
Hirschioporaceae	*Hirschioporus chinensis*	Dai 20264	China	OQ449101	OQ449204	OQ449127	OQ831443	OQ449017	[39]
Hirschioporaceae	*Hirschioporus chinensis*	Dai 21116	China	OQ437348	OQ438001	OQ448978	OQ831444	—	[39]
Hirschioporaceae	*Hirschioporus chinensis*	Dai 23048	China	OQ437349	OQ438002	OQ448979	OQ831445	OQ438032	[39]
Hirschioporaceae	*Hirschioporus floridanus*	Dolliner 640	USA	OQ437354	—	—	—	OQ438036	[39]
Hirschioporaceae	*Hirschioporus floridanus*	Dolliner 642	USA	OQ437355	OQ438004	—	—	OQ438037	[39]
Hirschioporaceae	*Hirschioporus floridanus*	MC1	Korea	MW795372	—	—	—	—	Genbank
Hirschioporaceae	*Hirschioporus fuscoviolaceus*	Dai 20988	Belarus	OQ437357	OQ438006	OQ448983	OQ831449	OQ438039	[39]
Hirschioporaceae	*Hirschioporus fuscoviolaceus*	Dai 21021	Belarus	OQ437360	OQ438009	OQ448986	OQ831451	—	[39]
Hirschioporaceae	*Hirschioporus fuscoviolaceus*	JV 1610/32	Czechia	MF381026	—	—	—	—	[36,39]
Hirschioporaceae	*"Hirschioporus fuscoviolaceus"*	Cui 11870	China	OQ437362	OQ438011	OQ448988	—	OQ438042	[39]
Hirschioporaceae	*"Hirschioporus fuscoviolaceus"*	Dai 10576	China	OQ437365	—	—	OQ831453	OQ438043	[39]
Hirschioporaceae	*"Hirschioporus fuscoviolaceus"*	Dai 22771	China	OQ437368	OQ438013	—	—	OQ438044	[39]
Hirschioporaceae	*"Hirschioporus fuscoviolaceus"*	V. Haikonen 25849	Finland	MF319119	MF318985	—	—	—	Genbank
Hirschioporaceae	*Hirschioporus montanus*	Cui 17067	China	OL470322	OL462836	OQ448990	OQ857930	OQ438048	[39]
Hirschioporaceae	*Hirschioporus montanus*	Dai 4204	China	OQ437376	OQ438018	OQ448996	OQ857936	OQ449151	[39]
Hirschioporaceae	*Hirschioporus montanus*	Dai 22979	China	OQ437372	OQ438015	OQ448991	OQ857931	OQ438049	[39]
Hirschioporaceae	*Hirschioporus montanus*	Dai 23143	China	OQ437374	OQ438016	OQ448993	OQ857933	OQ438051	[39]
Hirschioporaceae	*Hirschioporus pubescens*	Dai 17064	China	OQ437377	OQ438019	OQ448997	OQ857937	OQ449152	[39]
Hirschioporaceae	*Hirschioporus pubescens*	Dai 23710	China	OQ512026	OQ449059	OQ449169	OQ857938	OQ449153	[39]
Hirschioporaceae	*Hirschioporus pubescens*	KA17-0228	Korea	MN294864	—	—	—	—	[111]
Hirschioporaceae	*Hirschioporus pubescens*	SFC95081517	Korea	AF266680	—	—	—	—	[112]
Hirschioporaceae	*Hirschioporus pubescens*	SFC96060811	Korea	AF267644	—	—	—	—	[112]
Hirschioporaceae	*Hirschioporus pubescens*	SFC96102811	Korea	AF267645	—	—	—	—	[112]
Hirschioporaceae	*Hirschioporus* sp1	CCFC008387	Korea	AF266677	—	—	—	—	[112]
Hirschioporaceae	*Hirschioporus* sp1	CBS 374.68	Canada	AF266676	MH870875	AF408707	—	—	[107,112]
Hirschioporaceae	*Hirschioporus* sp1	UBCF20347	Canada	KC581332	—	—	—	—	Genbank
Hirschioporaceae	*Hirschioporus* sp1	UBCF28393	Canada	KP454016	—	—	—	—	Genbank
Hirschioporaceae	*Hirschioporus* sp2	CCFC01056	Canada	AF267647	—	—	—	—	[107,112]
Hirschioporaceae	*Hirschioporus* sp2	CBS 375.68	Canada	AF267648	MH870876	AF408716	—	—	[112]
Hirschioporaceae	*Hirschioporus tianschanicus*	Dai 15944	China	OQ437383	OQ449063	OQ449173	OQ857943	OQ449158	[39]
Hirschioporaceae	*Hirschioporus tianschanicus*	Dai 19067	China	OQ448960	OQ449067	OQ449177	OQ857947	OQ449162	[39]
Hirschioporaceae	*Hirschioporus tianschanicus*	Dai 19086	China	OQ448963	OQ449070	OQ449179	OQ857949	OQ449164	[39]
Hirschioporaceae	*Hirschioporus tianschanicus*	KA16-1050	Kyrgyzstan	MK351689	—	—	—	—	Genbank
Hirschioporaceae	*Nigrohirschioporus bulbocystidiatus*	Ryvarden 42922	Costa Rica	OQ448964	—	—	—	—	[39] Genbank
Hirschioporaceae	*Nigrohirschioporus confertus*	JV 1407/75	Costa Rica	MF380988	—	—	—	—	[36]

(to be continued)

Table 2. (continued)

Family	Species	Voucher	Locality	GenBank A accession no.					Ref.
				ITS	nLSU	mt-SSU	TEF1	nuc-SSU	
Hirschioporaceae	*Nigrohirschioporus confertus*	JV 1504/101	Costa Rica	MF380992	—	—	—	—	[36]
Hirschioporaceae	*Nigrohirschioporus confertus*	JV 1504/32	Costa Rica	MF380991	—	—	—	—	[36]
Hirschioporaceae	*Nigrohirschioporus deviatus*	Ryvarden 46959	Venezuela	OQ476081	—	—	—	—	[39]
Hirschioporaceae	*Nigrohirschioporus durus*	Cui 11327	China	OQ448965	OQ449071	OQ449180	OQ874781	OQ449165	[39]
Hirschioporaceae	*Nigrohirschioporus durus*	Dai 12305	China	OQ448969	OQ449073	—	OQ857951	OQ449167	[39]
Hirschioporaceae	*Nigrohirschioporus durus*	Dai 18419	Vietnam	OQ448970	—	—	—	—	[39]
Hirschioporaceae	*Nigrohirschioporus durus*	Dai 19497	Sri Lanka	OQ448971	OQ449074	OQ449181	OQ857952	OQ449168	[39]
Hirschioporaceae	*Nigrohirschioporus durus*	Dai 19640	Sri Lanka	OQ476082	OQ504233	OQ512031	OQ857953	OQ512030	[39]
Hirschioporaceae	*Nigrohirschioporus durus*	M1569	Japan	LC327032					[113]
Hirschioporaceae	*Nigrohirschioporus fissile*	TKC 145	Brazil	MK973088	—	—	—	—	Genbank
Hirschioporaceae	*Nigrohirschioporus fissile*	TKC 99	Brazil	MK973089	—	—	—	—	Genbank
Hirschioporaceae	*Nigrohirschioporus griseofuscus*	B3942	Brazil	OQ448975	OQ438022	—	OQ857957	OQ449106	[39]
Hirschioporaceae	*Nigrohirschioporus griseofuscus*	JV 1808/103	French Guiana	OQ448976	OQ438023	OQ449182	—	—	[39]
Hirschioporaceae	*Nigrohirschioporus griseofuscus*	JV 1909/6	French Guiana	OQ437343	OQ438024	—	OQ857958	OQ449107	[39]
Hirschioporaceae	*Nigrohirschioporus sector*	AS 2707	Brazil	OQ437344	OQ438025	OQ449183	OQ857959	OQ449108	[39]
Hirschioporaceae	*Nigrohirschioporus sector*	Dolliner 897	USA	OQ437346	—	—	—	—	[39]
Hirschioporaceae	*Nigrohirschioporus sector*	JV 1408/8-J	Costa Rica	OQ437347	OQ438027	—	OQ857961	—	[39]
Hirschioporaceae	*Nigrohirschioporus sector*	JV 1808/108	French Guiana	OQ453304	OQ453531	OQ453509	—	OQ453485	[39]
Hirschioporaceae	*Nigrohirschioporus keylargoensis*	JV 0904/66-J	USA	MF381009	PX747684	—	PX766002	PX747671	[36] and present study
Hirschioporaceae	*Nigrohirschioporus keylargoensis*	JV 2103/2-J	USA	PX741913	PX747685	—	PX766003	PX747672	Present study
Hirschioporaceae	*Nigrohirschioporus* sp1	CF00108	Thailand	OQ076496	—	—	—	—	[114]
Hirschioporaceae	*Nigrohirschioporus* sp1	NLB1300	Australia	ON715817	—	—	—	—	Genbank
Hirschioporaceae	*Nigrohirschioporus* sp1	NLB1301	Australia	ON715818	—	—	—	—	Genbank
Hirschioporaceae	*Nigrohirschioporus submurinus*	Dai 18392	Vietnam	OQ453305	OQ453532	—	—	OQ453486	[39]
Hirschioporaceae	*Nigrohirschioporus trimiticus*	B696	Brazil	OQ453308	OQ453535	—	—	OQ453488	[39]
Hirschioporaceae	*Nigrohirschioporus trimiticus*	B3471	Brazil	OQ453306	OQ453533	—	OQ857962	—	[39]
Hirschioporaceae	*Nigrohirschioporus trimiticus*	B4105	Brazil	OQ453307	OQ453534	OQ453510	OQ857963	OQ453487	[39]
Hirschioporaceae	*Nigrohirschioporus wuyiensis*	Dai 24990	China	PX741910	PX747682	PX747725	PX766000	PX747669	Present study
Hirschioporaceae	*Nigrohirschioporus wuyiensis*	Dai 24991	China	PX741911	PX747683	PX747726	PX766001	PX747670	Present study
Hirschioporaceae	*Pallidohirschioporus biformis*	Cui 7213	Japan	OQ453310	OQ453537	—	—	OQ453490	[39]
Hirschioporaceae	*Pallidohirschioporus biformis*	CZ 411	China	FJ755247	—	—	—	—	Genbank
Hirschioporaceae	*Pallidohirschioporus biformis*	Dai 12746	USA	OQ453311	OQ453538	OQ453512	OQ874735	OQ453491	[39]
Hirschioporaceae	*Pallidohirschioporus biformis*	Dai 16076	China	OQ453316	OQ453542	OQ453517	OQ874740	OQ453495	[39]
Hirschioporaceae	*Pallidohirschioporus biformis*	Dai 19466	China	OQ453223	OQ453548	OQ453523	OQ874743	OQ453501	[39]
Hirschioporaceae	*Pallidohirschioporus biformis*	Dai 20920	Belarus	OQ453226	OQ453282	OQ453526	OQ874745	OQ453504	[39]
Hirschioporaceae	*Pallidohirschioporus biformis*	He 2146	USA	OQ453230	OQ453286	OQ453529	OQ874747	OQ453507	[39]
Hirschioporaceae	*Pallidohirschioporus brastagii*	Dai 12316	China	OQ453235	OQ453289	OQ453268	OQ874749	OQ453246	[39]
Hirschioporaceae	*Pallidohirschioporus brastagii*	Dai 18804	Australia	OQ453236	OQ453290	OQ453269	—	OQ453247	[39]
Hirschioporaceae	*Pallidohirschioporus brastagii*	Dai 20459	China	OQ453240	OQ453294	OQ453271	—	OQ453249	[39]
Hirschioporaceae	*Pallidohirschioporus brastagii*	Dai 22919	China	OQ453371	OQ453297	OQ453274	OQ874751	OQ453251	[39]
Hirschioporaceae	*Pallidohirschioporus imbricatus*	Cui 5384	China	OQ453374	—	OQ453277	OQ874754	OQ453252	[39]

(to be continued)

Table 2. (continued)

Family	Species	Voucher	Locality	GenBank A accession no.					Ref.
				ITS	nLSU	mt-SSU	TEF1	nuc-SSU	
Hirschioporaceae	*Pallidohirschioporus polycystidiatus*	Dai 14686	China	OQ453377	OQ453300	OQ453278	OQ874756	OQ453254	[39]
Hirschioporaceae	*Pallidohirschioporus polycystidiatus*	Dai 19100	China	OQ453378	OQ453301	OQ453279	OQ874757	OQ453255	[39]
Hirschioporaceae	*Pallidohirschioporus polycystidiatus*	Dai 19103	China	OQ453380	OQ474949	OQ453281	OQ874759	OQ453257	[39]
Hirschioporaceae	*Pallidohirschioporus subchartaceus*	CCFC003932	USA	AF266679	—	AF408714	—	—	[112]
Hirschioporaceae	*Pallidohirschioporus subchartaceus*	JV 0509/146	USA	MF381010	—	—	—	—	[36]
Hirschioporaceae	*Pallidohirschioporus versicolor*	Cui 9701	China	OQ504334	OQ504324	OQ512029	OQ874760	OQ504328	[39]
Hirschioporaceae	*Pallidohirschioporus versicolor*	Cui 16974	China	OQ453383	OQ474950	OQ534100	—	OQ453259	[39]
Hirschioporaceae	*Pallidohirschioporus versicolor*	Dai 19331	China	OQ453386	OQ474951	—	OQ874762	OQ453261	[39]
Hirschioporaceae	*Pallidohirschioporus versicolor*	Dai 19332	China	OQ453387	OQ474952	OQ534102	OQ874763	OQ453262	[39]
Hirschioporaceae	*Pallidohirschioporus versicolor*	Dai 22867	China	OQ453390	OQ474954	OQ534105	OQ874766	OQ453265	[39]
Hirschioporaceae	*Perennihirschioporus agricola*	JV 1407/97	Costa Rica	MF380993	—	—	—	—	[36]
Hirschioporaceae	*Perennihirschioporus agricola*	JV 1504/75-J	Costa Rica	MF380995	—	—	—	—	[36]
Hirschioporaceae	*Perennihirschioporus daedaleus*	Cui 18235	Australia	OQ474938	—	OQ534106	OQ874767	OQ450175	[39]
Hirschioporaceae	*Perennihirschioporus daedaleus*	Dai 21143	Australia	OQ474939	—	—	—	—	[39]
Hirschioporaceae	*Perennihirschioporus fumosoavellaneus*	JV 1607/79-J	Costa Rica	MF381021	—	—	—	—	[36]
Hirschioporaceae	*Perennihirschioporus fumosoavellaneus*	JV 2203/80	Costa Rica	OQ474940	OQ474955	OQ512028	OQ874768	OQ450176	[39]
Hirschioporaceae	*Perennihirschioporus fumosoavellaneus*	JV 2203/85	Costa Rica	PX747736	—	—	—	—	Present study
Hirschioporaceae	*Perennihirschioporus perennis*	Dai 19295	China	OQ474941	OQ474956	—	OQ874779	—	[39]
Hirschioporaceae	*Perennihirschioporus* sp1	CBS 455.76	India	MH860992	MH872763	—	—	—	[107]
Hirschioporaceae	*Perennihirschioporus caymanensis*	JV 2208/7-J	French Guiana	PX741914	PX747686	PX747727	PX766004	PX747673	Present study
Hirschioporaceae	*Perennihirschioporus variabilis*	B856	Brazil	OQ474942	OQ474957	—	OQ874769	OQ450177	[39]
Hirschioporaceae	*Perennihirschioporus variabilis*	JV 1707/40-J	Mexico	OQ504335	OQ504325	OQ883911	OQ874770	—	[39]
Hirschioporaceae	*Perennihirschioporus variabilis*	Ryvarden 35177	Venezuela	OQ504337	—	—	—	—	[39]
Pseudotrichaptaceae	*Pseudotrichaptum laricinum*	ANT242-QFB28749	Canada	MN992532	—	—	—	—	Genbank
Pseudotrichaptaceae	*Pseudotrichaptum laricinum*	Dai 19455	China	—	OQ449019	—	—	OQ449394	[39]
Pseudotrichaptaceae	*Pseudotrichaptum laricinum*	Dai 19457	China	OQ449078	OQ449020	OQ517061	—	OQ449395	[39]
Pseudotrichaptaceae	*Pseudotrichaptum laricinum*	Dai 23782	China	OQ449079	OQ449021	OQ517062	—	OQ449396	[39]
Pseudotrichaptaceae	*Pseudotrichaptum laricinum*	RLG-4665	USA	U63471	—	—	—	—	[115]
Pseudotrichaptaceae	*Pseudotrichaptum laricinum*	YY 99	China	OQ449080	OQ449022	OQ517063	—	—	[39]
Podocarpioporaceae	*Podocarpioporus podocarpi*	Dai 12015	China	OQ449081	—	—	—	OQ449397	[39]
Podocarpioporaceae	*Podocarpioporus podocarpi*	Dai 21986	China	OQ449082	OQ449023	OQ517064	OQ785648	OQ449398	[39]
Podocarpioporaceae	*Podocarpioporus hydnoides*	Dai 26968	China	PX741918	PX747689	PX747730	PX766006	PX747676	Present study
Trichaptaceae	*Trichaptum byssogenum*	Dai 10753	China	OQ449083	OQ449024	OQ517065	—	OQ449399	[39]
Trichaptaceae	*Trichaptum byssogenum*	Dai 15555	China	OQ449085	OQ449026	OQ517067	OQ874771	OQ449401	[39]
Trichaptaceae	*Trichaptum byssogenum*	Dai 16758	Thailand	OQ449086	OQ449027	OQ517068	OQ874772	OQ449402	[39]
Trichaptaceae	*Trichaptum byssogenum*	Dai 18850	Australia	OQ449087	—	OQ517069	OQ874773	—	[39]
Trichaptaceae	*Trichaptum byssogenum*	E7361	Indonesia	AJ536654	—	—	—	—	Genbank
Trichaptaceae	*Trichaptum cystidiolatum*	JV 1512/18-J	Costa Rica	MF380996	—	—	—	—	[36]
Trichaptaceae	*Trichaptum cystidiolatum*	JV 2203/77	Costa Rica	PX741921	PX747690	PX747732	PX766008	PX747678	Present study
Trichaptaceae	*Trichaptum cystidiolatum*	JV 2203/78	Costa Rica	PX741922	PX747691	PX747733	PX766009	PX747679	Present study
Trichaptaceae	*Trichaptum perrottetii*	JV 1808/101	French Guiana	OQ449091	OQ449030	OQ517072	OQ874775	OQ449404	[39]
Trichaptaceae	*Trichaptum perrottetii*	JV 1908/45	French Guiana	OQ449092	OQ449031	—	OQ874776	OQ449405	[39]
Trichaptaceae	*Trichaptum perrottetii*	B2626	Brazil	OQ449093	OQ449032	—	OQ874777	OQ449406	[39]
Trichaptaceae	*Trichaptum resacarium*	JV 1109/56	USA	MF381020	—	—	—	—	[39]
Trichaptaceae	*Trichaptum resacarium*	JV 1109/57	USA	MF381018	—	—	—	—	[39]
Trichaptaceae	*Trichaptum strigosum*	JV 1012/2-J	USA	MF381011	—	OQ517073	OQ874778	—	[39]
Trichaptaceae	*Trichaptum longisporum*	JV 0809/19-J	Costa Rica	PX747737	—	—	—	—	Present study
Trichaptaceae	*Trichaptum longisporum*	JV 2203/104	Costa Rica	PX747738	—	—	—	—	Present study
Trichaptaceae	*Trichaptum longisporum*	JV 2311/13-J	Bolivia	PX741923	PX747692	PX747734	PX766010	PX747680	Present study
Trichaptaceae	*Trichaptum longisporum*	JV 2311/18-J	Bolivia	PX747739	—	—	—	—	Present study
Trichaptaceae	*Trichaptum longisporum*	JV 2311/19-J	Bolivia	PX741924	PX747693	PX747735	PX766011	PX747681	Present study

Note: '–' indicates that no sequence was obtained in this study.

sampling bias and spatial autocorrelation, the data were spatially thinned to match the resolution of the environmental variables, retaining only one occurrence record per 2.5 arc-min grid cell. Second, extreme outlier values were manually identified and removed by cross-referencing with explicit climatic distribution records documented in the literature. After these quality control measures, a final set of 25,828 valid distribution records for *Trichaptum* s.l. was established. The species of the genera were analyzed on a genus-by-genus basis to understand the key environmental factors influencing the distribution of each genus.

The maps were downloaded from the Natural Earth website (www.naturalearthdata.com) as the World Map (1:10 million scale). The collected geographic data of the generalized *Trichaptum* s.l. were processed and imported into ArcGIS software to create vector maps, ultimately producing the species' actual distribution map. Nineteen bioclimatic variables and elevation data with a spatial resolution of 2.5 arc-min were downloaded from the World Clim database (www.worldclim.org) (Table 3). These data were used to identify the primary environmental factors influencing the distribution of *Trichaptum* s.l. species, including baseline climate condition data averaged over the period from 1970 to 2000.

Results

The Phylogenetic relationships of *Trichaptum* s.l.

A total of 157 specimens of Dataset 1 (comprising 5,957 base pairs across five gene fragments) were used to reconstruct the phylogenetic relationships of *Trichaptum* s.l., including 148 specimens of *Trichaptum* s.l., three specimens of *Neoantrodiella*, four specimens of *Nigrofomes*, and two specimens of *Coltricia* as the outgroups[39]. Phylogenetic analyses were conducted using RAxML v. 8.2.12[70] and MrBayes v. 3.2.6[71], employing the best-fit model GTR + F + I + G4.

Phylogenetic inference resolved that *Trichaptum* s.l. is divided into four families: Hirschioporaceae, Pseudotrichaptaceae fam. nov., Podocarpioporaceae fam. nov., and Trichaptaceae (Fig. 1). The family Trichaptaceae forms a clade with Nigrofomitaceae and is closely related to Hirschioporaceae. Podocarpioporaceae is closely related to Neoantrodiellaceae, while Pseudotrichaptaceae is an independent clade within the order Hymenochaetales. Additionally, further analyses based on divergence times and morphological evidence were performed for the four families within *Trichaptum* s.l.

At the genus level, Hirschioporaceae comprises the most genera, including *Hirschioporus*, *Nigrohirschioporus*, *Pallidohirschioporus*, and *Perennihirschioporus*, while Pseudotrichaptaceae, Podocarpioporaceae, and Trichaptaceae each contain a single genus, namely *Pseudotrichaptum*, *Podocarpioporus*, and *Trichaptum*, respectively. All genera were recovered as monophyletic.

Phylogenetic analyses also revealed six new species described in this study, *Nigrohirschioporus keylargoensis* sp. nov., *Nigrohirschioporus wuyiensis* sp. nov., *Perennihirschioporus caymanensis* sp. nov., *Podocarpioporus hydnoides* sp. nov., *Trichaptum cystidiolatum* sp. nov., and *Trichaptum longisporum* sp. nov. (Fig. 1). *Nigrohirschioporus keylargoensis* is most closely related to *N. griseofuscus*, with strong support (96/1.00 in ML and BI analyses). *Nigrohirschioporus wuyiensis* is closely related to *N. submiurinus*, with strong support (99/1.00 in ML and BI analyses). *Perennihirschioporus caymanensis* is closely related to *P. fumosoavellaneus*, with moderate support (72/0.90 in ML and BI analyses). *Podocarpioporus hydnoides* is closely related to *P. podocarpi*, with full support (100/1.00 in ML and BI analyses). *Trichaptum cystidiolatum* is most closely related to *Trichaptum longisporum*, with full support (100/1.00 in ML and BI analyses).

In addition, five putative species represented by single specimens, "*Hirschioporus abietinus*", "*Hirschioporus fuscoviolaceus*", *Hirschioporus* sp 1, *Hirschioporus* sp 2, and *Nigrohirschioporus* sp 1, require further sampling for formal description.

Divergence times of *Trichaptum* s.l.

The dataset 2 (comprising 4,320 characters from three gene fragments) was used to estimate the divergence times of *Trichaptum* s.l. using Beast software v. 2.6.6[72] (Table 4). The results indicated that with the following mean stem ages (Fig. 2) the Basidiomycota and Ascomycota diverged at approximately 449 Mya with a 95% highest posterior density (HPD) of 406–554 Mya, the Agaricomycetes diverged around 330 Mya with a 95% HPD of 287–371 Mya, the Agaricales at 156 Mya with a 95% HPD of 121–196 Mya, and the Hymenochaetales at 247 Mya with a 95% HPD of 213–284 Mya. In addition, the mean stem ages of families within the order Hymenochaetales ranged from 71 Mya to 219 Mya.

Within *Trichaptum* s.l., the mean stem ages of the four families ranged from 71 Mya (with a 95% HPD of 42–102 Mya) for Pseudotrichaptaceae to 116 Mya (with a 95% HPD of 73–119 Mya) for Hirschioporaceae, during the Cretaceous period. The mean stem ages for Podocarpioporaceae and Trichaptaceae were 109 Mya (with a 95% HPD of 72–147 Mya) and 96 Mya (with a 95% HPD of 70–125 Mya), respectively. The mean stem ages for genera and species within *Trichaptum* s.l. were 71–96 Mya and 1–71 Mya, respectively. In

Table 3. Environmental variables used to create the species distribution model

	Description	Unit
Bio1	Annual mean temperature	°C
Bio2	Mean diurnal range (mean of monthly (max tempmin temp))	°C
Bio3	Isothermality (Bio2/Bio7) (× 100)	C of V
Bio4	Temperature seasonality (standard deviation × 100)	°C
Bio5	Maximum temperature of warmest month	°C
Bio6	Minimum temperature of coldest month	°C
Bio7	Temperature annual range (Bio5-Bio6)	°C
Bio8	Mean temperature of wettest quarter	°C
Bio9	Mean temperature of driest quarter	°C
Bio10	Mean temperature of warmest quarter	°C
Bio11	Mean temperature of coldest quarter	°C
Bio12	Annual precipitation	mm
Bio13	Precipitation of wettest month	mm
Bio14	Precipitation of driest month	mm
Bio15	Precipitation seasonality (coefficient of variation)	C of V
Bio16	Precipitation of wettest quarter	mm
Bio17	Precipitation of driest quarter	mm
Bio18	Precipitation of warmest quarter	mm
Bio19	Precipitation of coldest quarter	mm
Bio20	Elevation	m

Table 4. The estimated divergence times of *Trichaptum* s.l.

Family	Genus	Means of stem age (Mya)	95% HPD (Mya)
Hirschioporaceae		116	73–119
	Hirschioporus	75	55–97
	Nigrohirschioporus	74	52–97
	Pallidohirschioporus	75	55–97
	Perennihirschioporus	74	52–97
Pseudotrichaptaceae		71	42–102
	Pseudotrichaptum	71	42–102
Podocarpioporaceae		109	72–147
	Podocarpioporus	109	72–147
Trichaptaceae		96	70–125
	Trichaptum	96	70–125

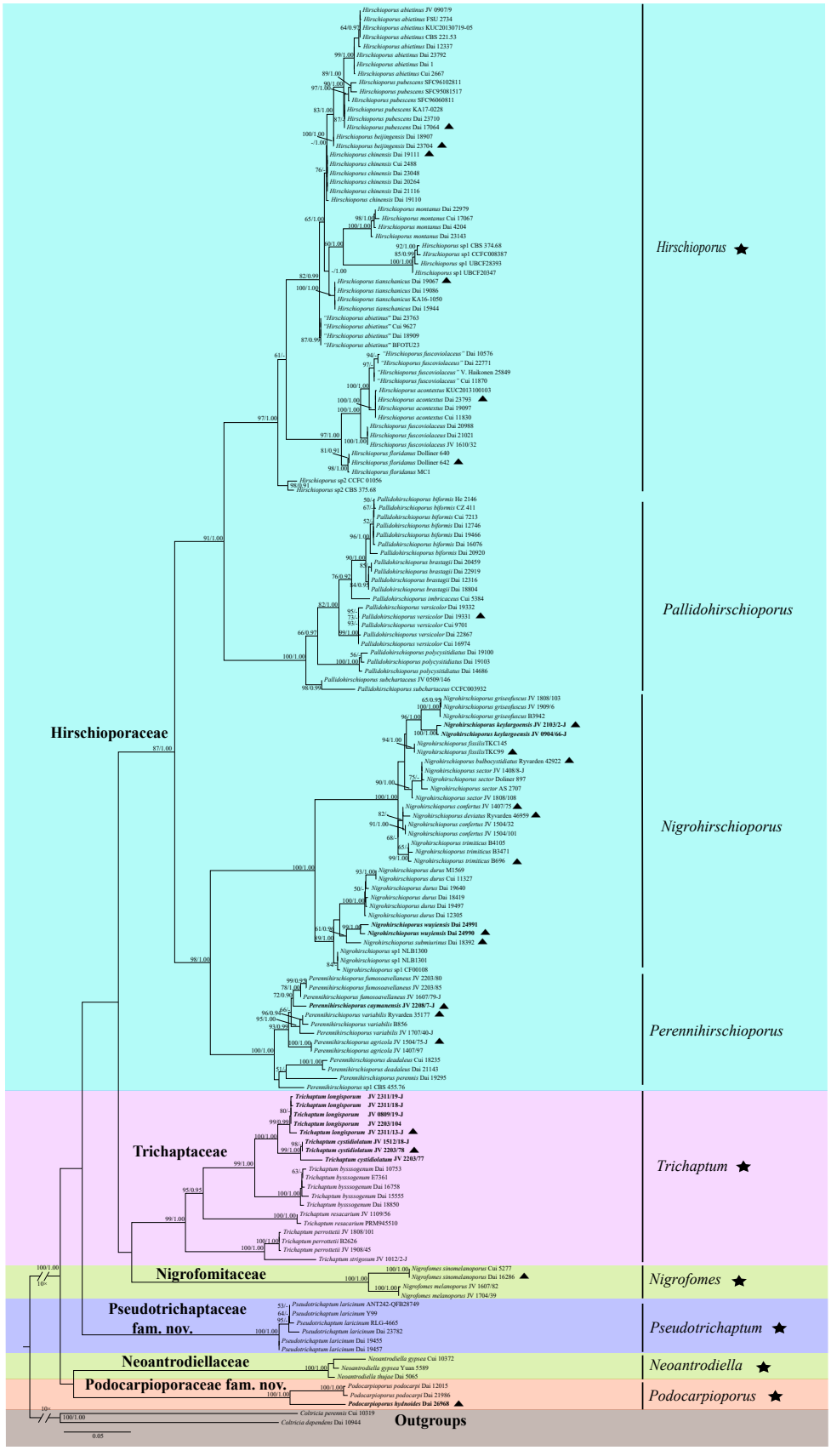

Fig. 1 Maximum Likelihood (ML) tree of *Trichaptum* s.l. was constructed based on five sequences (ITS, nLSU, TEF1, mt-SSU, and nuc-SSU), using *Coltricia dependens* and *C. perennis* as outgroups. ML bootstrap values (≥ 50%) and Bayesian inference (BI) posterior probabilities (≥ 0.9) are shown along the branches for each clade. The six new species, *Nigrohirschioporus keylargoensis*, *N. wuyiensis*, *Perennihirschioporus caymanensis*, *Podocarpioporus hydnoides*, *Trichaptum cystidiolatum*, and *T. longisporum*, are highlighted in bold. A scale bar in the upper left represents substitutions per site. Black stars (★) represent type genera, and black triangles (▲) represent type sequences.

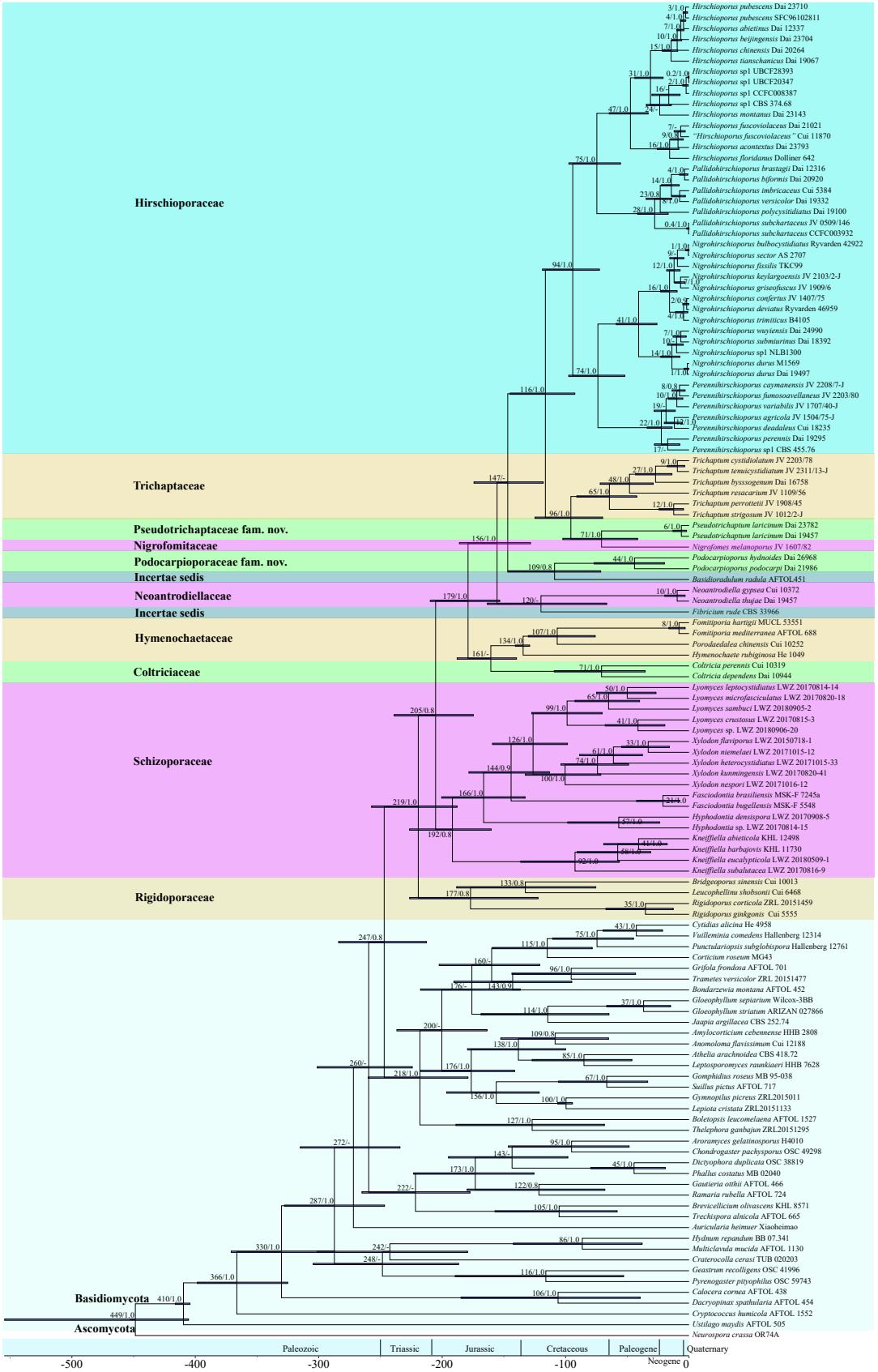

Fig. 2 The estimated divergence times for the *Trichaptum* s.l. are shown, derived from molecular clock analyses using three sequences (ITS, nLSU, and TEF1). Mean divergence times (Mya) and posterior probabilities (PP) > 0.8 are annotated at the internodes, with horizontal blue bars representing the 95% highest posterior density (HPD) intervals for divergence time estimates.

this study, with the exception of *Pseudotrichaptum laricinum*, all other species diverged starting in the Eocene period (1–48 Mya).

Taxonomy

In this study, two new families, Pseudotrichaptaceae and Podocarpioporaceae, and six new species of *Trichaptum* s.l. within the Hymenochaetales are proposed *Nigrohirschioporus keylargoensis*, *N. wuyiensis*, *Perennihirschioporus caymanensis*, *Podocarpioporus hydnoides*, *Trichaptum cystidiolatum*, and *T. longisporum*. These proposals are supported by phylogenetic, divergence time, and morphological evidence.

Key to families of Trichaptum s.l

1.	Cystidia projecting out of the hymenium, apically often with long rectangular yellowish crystals; cystidia length usually more than twice that of basidia; restricted to *Podocarpus*	Podocarpioporaceae
1.	Cystidia usually within the hymenium, apically with hyaline crystals; cystidia similar in length to basidia	2
2.	Hymenophore lamellate, completely without pores; growing on gymnosperm wood	Pseudotrichaptaceae
2.	Hymenophore poroid or hydnoid, poroid at least when young or at the margin; growing on angiosperm and gymnosperm wood	3
3.	Upper surface glabrous to adpressed tomentose, mixed with glabrous zones; cystidia mostly fusoid, clavate to capitate	Trichaptaceae
3.	Upper surface strongly strigose to hispid; cystidia mostly subulate to ventricose	Hirschioporaceae

Pseudotrichaptaceae Meng Zhou, Y.J. Cui, H. Zhao, Y.C. Dai & Yuan Yuan, fam. nov.

MycoBank number: MB 862003

Type genus – *Pseudotrichaptum* Y.C. Dai, Yuan Yuan & Meng Zhou, Mycosphere 14(1): 890 (2023)

Type species – *Pseudotrichaptum laricinum* (P. Karst.) Y.C. Dai, Yuan Yuan & Meng Zhou, Mycosphere 14(1): 890 (2023)

Key characteristics: Basidiomata annual, pileate or effused-reflexed, coriaceous to tough; pileal surface cream to pale buff with distinct concentric sulcate zones, covered by mosses with age; hymenophore lamellate; lamella purplish, thin, entire and wavy, dichotomously forked near margin; context duplex. Hyphal system dimitic; generative hyphae with clamp connections, skeletal hyphae pale yellowish in KOH, IKI–, CB+; cystidia apically encrusted; basidiospores allantoid, IKI–, CB–.

Notes: Pseudotrichaptaceae is distinguished from other families in *Trichaptum* s.l. by its coriaceous pilei with purplish lamellate hymenophore and primarily inhabit coniferous trees with a circumboreal distribution in the Northern Hemisphere.

Podocarpioporaceae Meng Zhou, Y.J. Cui, H. Zhao, Y.C. Dai & Yuan Yuan, fam. nov.

MycoBank number: MB 862004

Type genus – *Podocarpioporus* Y.C. Dai, Yuan Yuan & Meng Zhou, Mycosphere 14(1): 888 (2023)

Type species – *Podocarpioporus podocarpi* (Y.C. Dai) Y.C. Dai, Yuan Yuan & Meng Zhou, Mycosphere 14(1): 889 (2023)

Key characteristics: Basidiomata annual, resupinate or effused-reflexed to pileate; hymenophore poroid to irpicoid. Hyphal system dimitic; generative hyphae with clamp connections; skeletal hyphae occasionally with simple septa, IKI–, CB+; tissue darkening but otherwise unchanged in KOH. Cystidia encrusted at the apex or not; basidiospores allantoid, hyaline, thin-walled, smooth, IKI–, CB–.

Notes: This family is unique in *Trichaptum* s.l. because of the poroid to irpicoid hymenophore, narrow allantoid basidiospores, distinctly long subulate hymenial cystidia, usually more than twice that of basidia, and growth only on species of Podocarpaceae.

Nigrohirschioporus keylargoensis Meng Zhou, Y.C. Dai, H. Zhao, Vlasák & Yuan Yuan sp. nov. (Figs 3, 4)

MycoBank number: MB 361999

Type – USA. Florida, Key Largo, on fallen angiosperm trunk, III.2021, JV 2103/2-J (Holotype BJFC039885).

Etymology – *Keylargoensis* (Lat.): refers to the type locality, Key Largo, Florida, USA.

Basidiomata – Annual, effused-reflexed to pileate; corky when fresh and dry. Pilei semicircular to elongate, flexible and tough, projecting up to 3 cm, 3 cm wide and 3 mm thick at the base. Pileal surface pale fuscous, vinaceous or vinaceous buff to snuff brown when fresh and honey yellow to fuscous when dry, finely tomentose to velutinate, sub-scaly towards the margin; margin entire to lobed. Hymenophore poroid to irpicoid or hydnoid, olivaceous buff when fresh, grayish brown to fuscous when dry; pores angular when juvenile, becoming split to dentate with age, 1–2 per mm; dissepiments thin, entire when juvenile, strongly lacerate with age. Context duplex, up to 1.5 mm thick, the upper layer grayish brown, pubescent, soft, up to 1 mm, the lower layer coriaceous dark brown, tubes brown, up to 2 mm long.

Hyphal structure – Hyphal system trimitic; generative hyphae with clamp connections, hyaline, thin-walled; skeletal hyphae thick-walled with a narrow lumen, slightly dextrinoid, CB+; binding hyphae thick-walled to sub-solid; tissues darkening in KOH.

Context – Generative hyphae hyaline, thin-walled, occasionally branched, 2.5–3 μm in diam.; skeletal hyphae thick-walled with a narrow lumen, unbranched, regularly arranged, 4–6 μm in diam.; binding hyphae thick-walled with a narrow lumen, rarely branched, interwoven, 1.5–2.5 μm in diam.

Tubes – Generative hyphae hyaline, thin-walled, occasionally branched, 2.5–3 μm in diam.; skeletal hyphae thick-walled, unbranched, interwoven, 3–5 μm in diam; binding hyphae thick-walled with a narrow lumen to sub-solid, rarely branched, interwoven, 1.5–2 μm in diam.

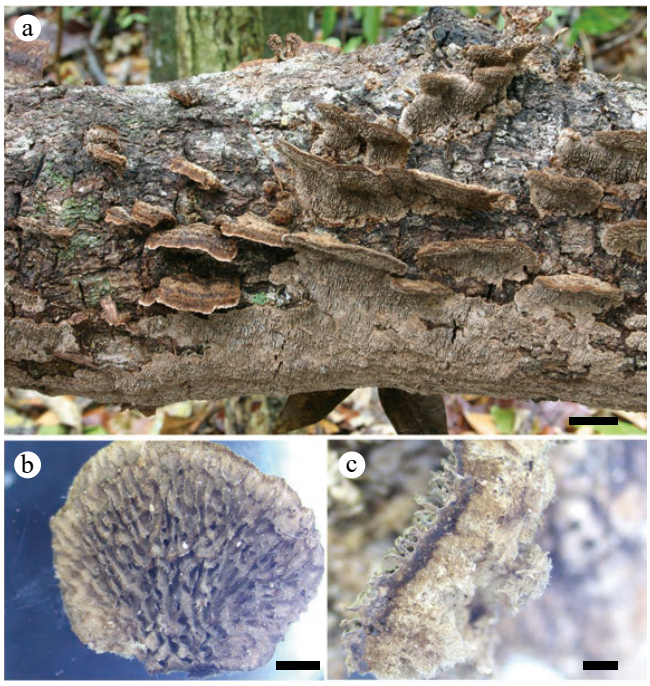

Fig. 3 Basidiomata of *Nigrohirschioporus keylargoensis* JV0904/66-J. Scale bars: (a) = 1 cm, (b) and (c) = 1 mm.

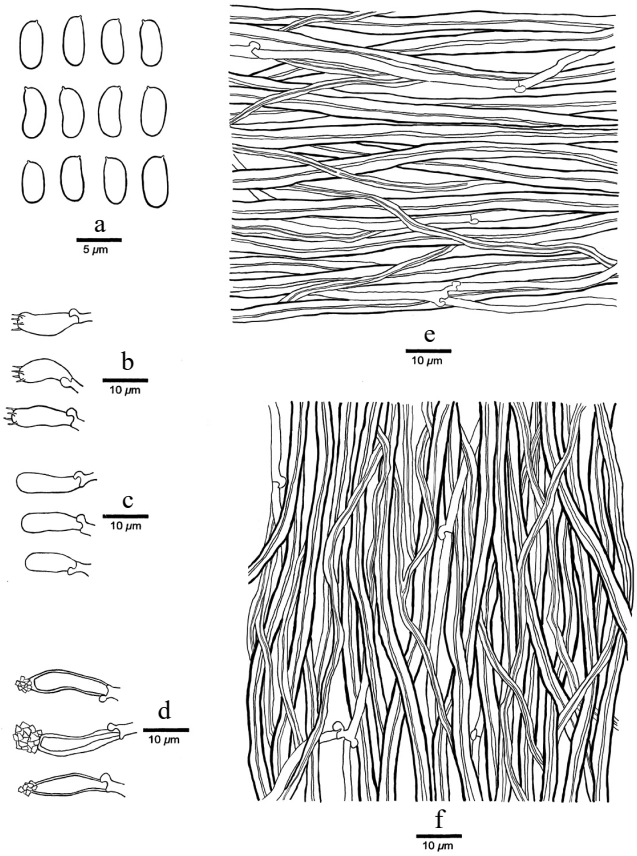

Fig. 4 Microscopic structures of *Nigrohirschioporus keylargoensis* (drawn from the holotype, JV0904/66-J). (a) Basidiospores. (b) Basidia. (c) Basidioles. (d) Cystidia. (e) Hyphae from context. (f) Hyphae from trama.

Hymenium – Cystidia fusoid to capitate, slightly thick-walled, abundant, sometimes apically encrusted, 15–25 × 4–6 μm; hyphal pegs absent; basidia clavate, with four sterigmata and a basal clamp connection, 13–18 × 4.5–6 μm; basidioles similar with basidia in shape, but smaller.

Spores – Basidiospores cylindric to slightly allantoid, hyaline, thin-walled, smooth, IKI–, CB–, (5.0–)5.1–7.0(–7.1) × (1.9–)2–3(–3.2) μm, L = 5.95 μm, W = 2.41μm, Q = 2.03–2.95 (n = 60/2).

Type of rot – White rot.

Distribution and ecology – *Nigrohirschioporus keylargoensis* has so far only been found in Florida, USA.

Specimens examined – USA. Florida, Key Largo, on a fallen angiosperm trunk, IV.2009, JV0904/66-J (BJFC039884); III.2021, JV 2103/2-J (holotype BJFC039885).

Nigrohirschioporus wuyiensis Meng Zhou, Y.J. Cui, H. Zhao, Y.C. Dai & Yuan Yuan, sp. nov. (Figs 5,6)

MycoBank number: MB 361998

Type – CHINA. Zhejiang, Wuyi, on fallen branch of *Liquidambar*, 18.VI.2023, Dai 24990 (Holotype BJFC042543).

Etymology – *Wuyiensis* (Lat.): refers to the species being found in Wuyi, Zhejiang Province in China.

Basidiomata – Annual, resupinate; corky when fresh, becoming brittle upon drying, up to 5 cm long, 2 cm wide, and 3 mm thick at the center. Hymenophore poroid, olivaceous buff when fresh, buff to clay buff when dry; pores angular when juvenile, becoming irpicoid with age, 4–6 per mm; dissepiments thin, entire when juvenile, strongly lacerate with age. Context buff-yellow when dry, up to 0.5 mm thick. Tubes pale buff, up to 2.5 mm long.

Hyphal structure – Hyphal system dimitic; generative hyphae with clamp connections, hyaline, slightly thick-walled; skeletal hyphae distinctly thick-walled, slightly dextrinoid, CB+; tissues darkening in KOH.

Context – Generative hyphae hyaline, slightly thick-walled, rarely branched, 2–3.5 μm in diam.; skeletal hyphae thick-walled with a wide lumen, unbranched, interwoven, 3–4 μm in diam.

Tubes – Generative hyphae hyaline, slightly thick-walled, rarely branched, usually covered by abundant fine thorn-like crystals, 2.5–3.5 μm in diam.; skeletal hyphae thick-walled, unbranched, interwoven, 3–5 μm in diam.

Hymenium – Cystidia clavate to fusoid, thin-walled, abundant, sometimes apically encrusted, 17–25 × 4.5–6 μm; hyphal pegs present; basidia clavate, with four sterigmata and a basal clamp connection, 16.5–26 × 5.5–7 μm; basidioles similar to basidia in shape, but smaller.

Spores – Basidiospores cylindric to slightly allantoid, hyaline, thin-walled, smooth, IKI–, CB–, (5–)5.5–7.2(–7.3) × 2–2.5(–2.8) μm, L = 6.47 μm, W = 2.27 μm, Q = 2.79–2.92 (n = 60/2).

Type of rot – White rot.

Distribution and ecology – *Nigrohirschioporus wuyiensis* has so far only been found in Zhejiang, subtropical China.

Specimens examined – CHINA. Zhejiang, Wuyi, on a fallen branch of *Liquidambar*, 18.VI.2023, Dai 24990 (holotype BJFC042543); Dai 24991 (BJFC042544).

Key to known species of Nigrohirschioporus

1.	Basidiomata perennial	2
1.	Basidiomata annual	5
2.	Basidiomata resupinate	*N. deviatus*
2.	Basidiomata effused-reflexed to pileate	3
3.	Pores 5–8 per mm	*N. nigrivineus*
3.	Pores > 8 per mm	4
4.	Pore surface pale orange, pores 13–16 per mm	*N. agglutinatus*
4.	Pore surface dark purplish to grayish brown, pores 8–10 per mm	*N. durus*
5.	Basidiomata completely resupinate	6
5.	Basidiomata resupinate to effused-reflexed or pileate	8
6.	Hymenophore poroid to irpicoid, pores 2–4 per mm	*N. bulbocystidiatus*
6.	Hymenophore poroid, pores 4–9 per mm	7
7.	Pores 6–9 per mm; cystidia fusoid with a long neck	*N. submurinus*
7.	Pores 4–6 per mm; cystidia clavate to fusoid	*N. wuyiensis*
8.	Hymenophore hydnoid to irpicoid	9
8.	Hymenophore poroid	11
9.	Hyphal system dimitic	*N. griseofuscus*
9.	Hyphal system trimitic	10
10.	Spores broadly ellipsoid, 4–4.8 × 3–3.5 μm	*N. molestus*
10.	Spores cylindric, slightly curved, 5.1–7 × 2–3 μm	*N. keylargoensis*
11.	Hyphal system trimitic	12
11.	Hyphal system dimitic	13
12.	Spores ellipsoid, 4–4.5 × 1.8–2.2 μm	*N. confertus*
12.	Spores cylindric to slightly allantoid, 5–6 × 2.4–2.7 μm	*N. trimiticus*
13.	Basidiospores cylindrical, 6.4–10 × 2.3–3.2 μm	*N. fissilis*
13.	Basidiospores narrowly ellipsoid, 5–6.4 × 2.2–2.5 μm	*N. sector*

Perennihirschioporus caymanensis Meng Zhou, H. Zhao, Vlasák, Y.C. Dai & Yuan Yuan, sp. nov. (Figs 7,8)

MycoBank number: MB 861997

Type – FRENCH GUIANA, Camp Cayman, ravine, on dead stump of extremely hard, dark "ironwood", 25.VIII.2022, JV 2208/7-J (Holotype BJFC044766).

Etymology – *Caymanensis* (Lat.): refers to the species being found in Camp Cayman, French Guiana.

Basidiomata – Perennial, pileate, solitary, consistency hard, corky to woody; pilei applanate, projecting up to 10 cm, 10 cm wide, and

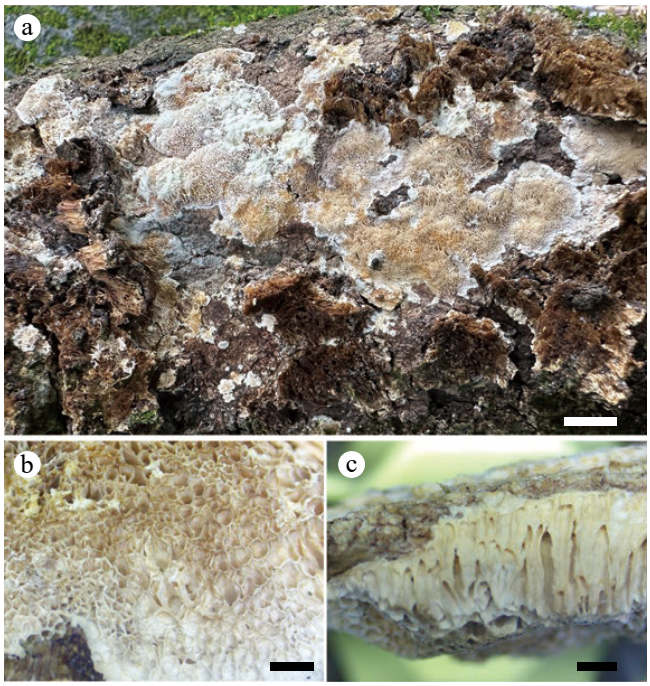

Fig. 5 Basidiomata of *Nigrohirschioporus wuyiensis* Dai 24990 (holotype). Scale bars: (a) = 1 cm, (b) and (c) = 1 mm.

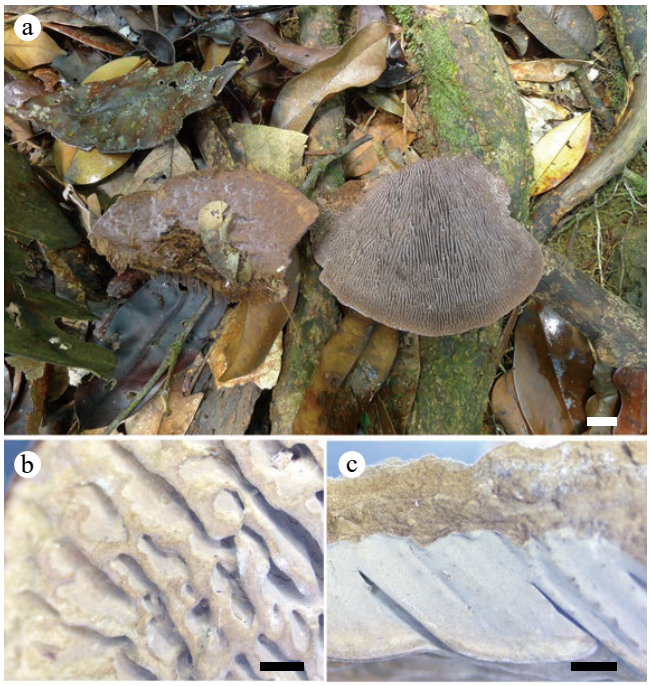

Fig. 7 Basidiomata of *Perennihirschioporus caymanensis* JV 2208/7-J (holotype). Scale bars: (a) = 1 cm, (b) and (c) = 1 mm.

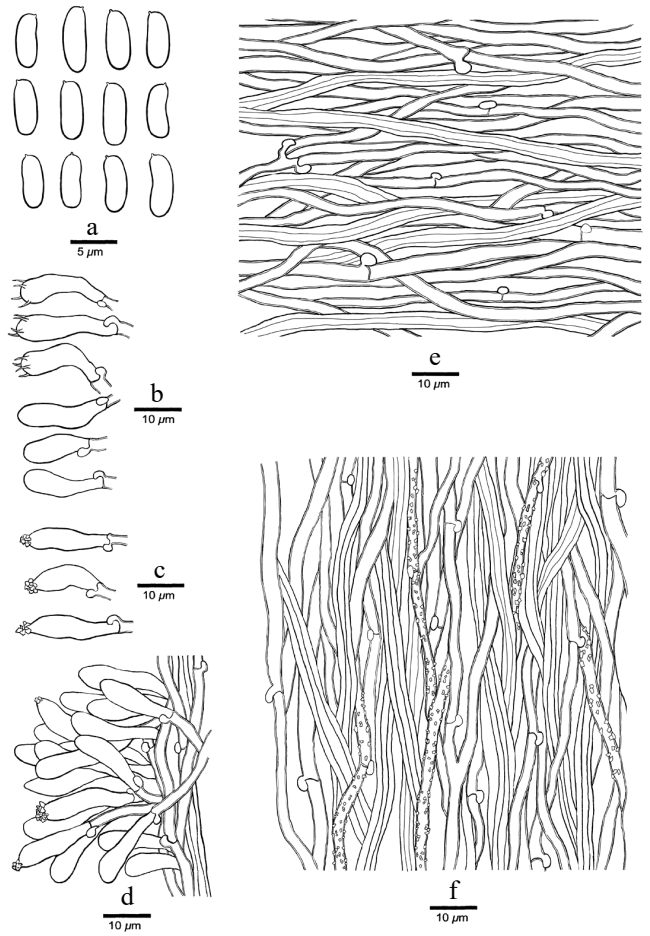

Fig. 6 Microscopic structures of *Nigrohirschioporus wuyiensis* (drawn from the holotype, Dai 24990). (a) Basidiospores. (b) Basidia and basidioles. (c) Cystidia. (d) Hyphal peg. (e) Hyphae from context. (f) Hyphae from trama.

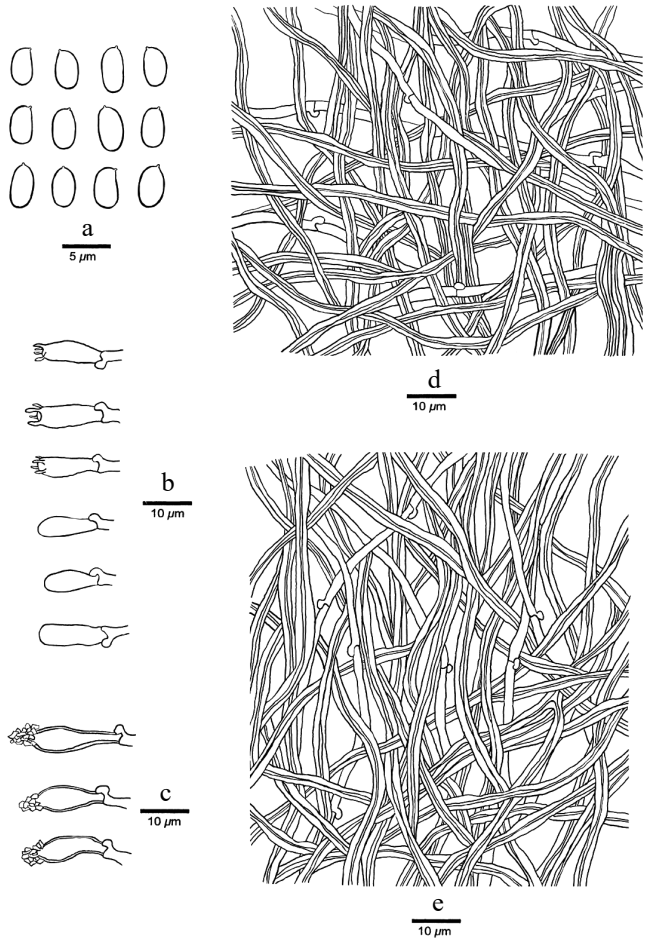

Fig. 8 Microscopic structures of *Perennihirschioporus caymanensis* (drawn from the holotype, JV 2208/7-J). (a) Basidiospores. (b) Basidia and basidioles. (c) Cystidia. (d) Hyphae from context. (e) Hyphae from trama.

1.5 cm thick at base. Pileal surface brownish with a distinct violet tint when fresh and umber when dry, hairless, rough, slightly warted; margin brown, acute, entire. Hymenophore daedaleoid to lamellate, dark brown when fresh and grayish brown to dark brown when dry; pores or lamella 0.5–2 per mm, radially elongate or daedaleoid near the margin; dissepiments wavy, thick, entire. Sterile margin indistinct. Context homogeneous, brown, hard corky, up to 4 mm thick. Tubes concolorous with context, up to 11 mm long.

Hyphal structure – Hyphal system dimitic; generative hyphae with clamp connections, hyaline, thin-walled; skeletal hyphae dominant, yellowish, distinctly thick-walled with a narrow lumen, IKI–, CB+; tissues darkening in KOH.

Context – Generative hyphae hyaline, thin-walled, unbranched, 2–3 μm in diam.; skeletal hyphae thick-walled with a narrow lumen, unbranched, interwoven, 2–3 μm in diam.

Tubes – Generative hyphae hyaline, thin-walled, unbranched, 1.5–2.7 μm in diam.; skeletal hyphae thick-walled with a narrow lumen, rarely branched, interwoven, 2.5–4.5 μm in diam.; hyphae at dissepiment edges are smooth.

Hymenium – Cystidia fusoid, slightly thick-walled, abundant, usually apically encrusted, 17–25 × 4–5.5 μm, projecting outside of hymenium up to 7 μm, with a basal clamp connection; hyphal pegs absent; basidia clavate with four sterigmata and a basal clamp connection, 12–15 × 4.5–5.0 μm, basidioles similar to basidia in shape, but slightly smaller.

Spores – Basidiospores oblong ellipsoid to ellipsoid, hyaline, thin-walled, smooth, IKI–, CB–, (3.2–)3.5–4.3(–4.5) × (1.9–)2–2.7 μm, L =3.85 μm, W = 2.28μm, Q =1.69 (n=30/1)

Type of rot – White rot.

Distribution and ecology – *Perennihirschioporus caymanensis* is known from the type locality only, where several basidiomata were growing on a dead standing tree. After four years, in 2026, the fresh fungus was still growing in many pilei on the stag which indicates high subdtrate resistance to decay.

Specimens examined – FRENCH GUIANA, Camp Cayman, ravine, 25.VIII.2022, JV 2208/7-J (Holotype BJFC044766); 15.II.2026, JV 2602/8 (JV, PRM).

Key to known species of Perennihirschioporus

1.	Hymenophore irpicoid, daedaleoid to lamellate	2
1.	Hymenophore poroid	4
2.	Basidiomata effused-reflexed to pileate or resupinate	*P. variabilis*
2.	Basidiomata pileate	3
3.	Basidiomata applanate, hymenophore daedaleoid to lamellate	*P. caymanensis*
3.	Basidiomata triquetrous, hymenophore daedaleoid to hydnoid	*P. daedaleus*
4.	Basidiomata effused-reflexed to pileate, pore surface vinaceous brown to umber; hyphal system dimitic	*P. perennis*
4.	Basidiomata completely pileate, pore surface pale brown to avellaneus; hyphal system trimitic	5
5.	Pores 1–3 per mm; basidiospores 4–5 × 2.5–3 μm	*P. agricola*
5.	Pores 3–4 per mm; basidiospores 3.6–4 × 2.5–3 μm	*P. fumosoavellaneus*

Trichaptum cystidiolatum Meng Zhou, H. Zhao, Y.J. Cui Vlasák, Y.C. Dai & Yuan Yuan, sp. nov. (Figs 9,10)

MycoBank number: MB 861996

Type – COSTA RICA. Rincón de la Vieja, Guachipelin, on hardwood, III. 2022, JV2203/78 (Holotype BJFC044764).

Etymology – *Cystidiolatum* (Lat.): refers to the presence of cystidioles.

Basidiomata – Perennial, effused-reflexed or resupinate; corky when fresh, hard corky when dry. Pilei are sometimes laterally fused, projecting up to 2 cm, 4 cm wide, and 4 mm thick at the base. Pileal surface consistently whitish, ochraceous to milky coffee when fresh

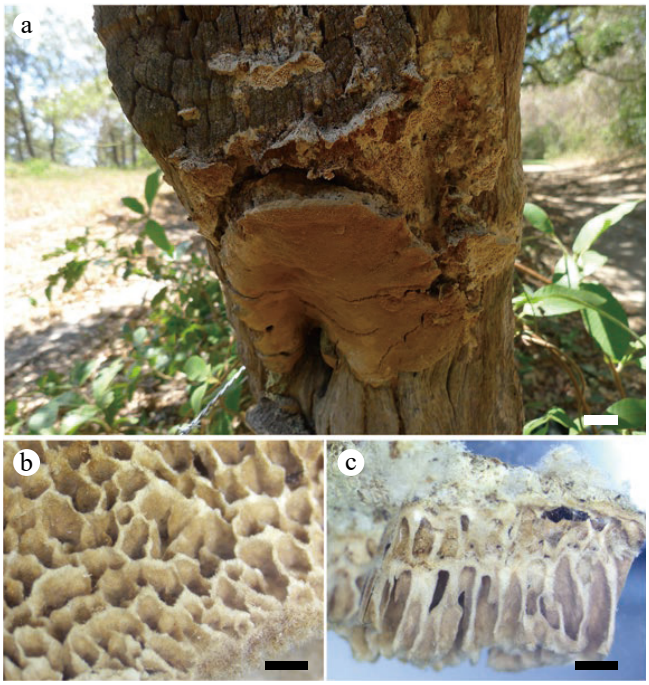

Fig. 9 Basidiomata of *Trichaptum cystidiolatum* JV 2203/78 (holotype). Note: JV 2203/78 is the whitish, eff-reflexed, large-pores *Poria* growing around the central, brown and massive fruitbody of *P. agricola*. Scale bars: (a) = 1 cm, (b) and (c) = 1 mm.

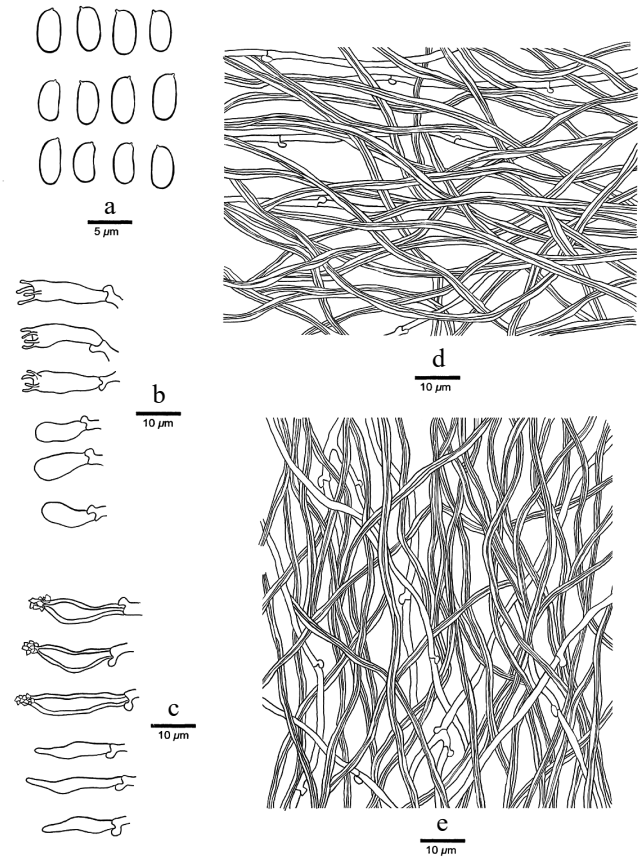

Fig. 10 Microscopic structures of *Trichaptum cystidiolatum* (drawn from the holotype, JV 2203/78). (a) Basidiospores. (b) Basidia and basidioles. (c) Cystidia and cystidioles. (d) Hyphae from context. (e) Hyphae from trama.

and milky coffee when dry, adpressed velutinate; margin sharp, entire to lobed. Hymenophore poroid, whitish ochre when dry and pale buff when old; pores angular, 1–3 per mm; dissepiments thin, entire. Context gray to ochraceous or milky coffee, thin, up to 0.3 mm. Tubes concolorous with context, up to 2 mm long.

Hyphal structure – Hyphal system dimitic; generative hyphae with clamp connections, hyaline, thin-walled; skeletal hyphae distinctly thick-walled to subsolid, slightly dextrinoid, CB–; tissues unchanged in KOH.

Context – Generative hyphae hyaline, thin-walled, occasionally branched, 1–2 μm in diam.; skeletal hyphae thick-walled with a narrow lumen to subsolid, unbranched, interwoven, 1.5–2.5 μm in diam.

Tubes – Generative hyphae hyaline, thin-walled, usually branched, 1.5–2 μm in diam.; skeletal hyphae thick-walled with a wide lumen, unbranched, interwoven, 1.5–2 μm in diam.

Hymenium – Cystidia fusoid, thick-walled, apically encrusted, sometimes with several separate, 16–26 × 3–6 μm, cystidioles narrow fusoid, thin-walled, 14–22 × 3-4; hyphal pegs absent; basidia barrel-shaped, with four sterigmata and a basal clamp connection, 16–22 × 4.5–6 μm; basidioles similar with basidia in shape, but smaller.

Spores – Basidiospores oblong ellipsoid, hyaline, thin-walled, smooth, IKI–, CB–, (4.2–)4.5–6(–6.5) × (2–) 2.2–2.9 μm, L = 5.31μm, W = 2.56 μm, Q = 2.02–2.13 (n = 30/2).

Type of rot – White rot.

Distribution and ecology – To date, *Trichaptum cystidiolatum* is found in Costa Rica only, where it is locally not rare on wooden fence posts.

Specimens examined – COSTA RICA. Guanacaste Prov., Rincón de la Vieja, Guachipelin, on angiosperm wood of fence posts, 12.III. 2022, JV2203/77 (BJFC044763), JV2203/78 (holotype BJFC044764), JV2203/101; Santa Cruz, fallen angiosperm branch, 28.XII. 2015, JV1512/18-J (JV, PRM 945507, GenBank MF380996).

Trichaptum longisporum Meng Zhou, Y.J. Cui, H. Zhao, Vlasák, Y.C. Dai & Yuan Yuan, sp. nov. (Figs 11,12)

MycoBank number: MB 861995

Type – BOLIVIA. St. Cruz Dept., Refugio los Volcanes, on angiosperm stump, XI.2023, JV 2311/13-J (Holotype BJFC044759).

Etymology – *Longisporum* (Lat.): refers to the species having distinct long basidiospores.

Basidiomata – Perennial, pileate, sometimes resupinate; corky when fresh, hard corky when dry. Pilei applanate, usually imbricate or several specimens broadly attached to fused laterally in rows, projecting up to 2 cm, 6 cm wide, and 8 mm thick at base. Pileal surface distinctly flesh pink to rose when fresh, pinkish buff to grayish brown when dry, concentrically sulcate and radially striate, hispid to tomentose, more adpressed along the margin, faintly zonate; margin sharp, entire. Hymenophore poroid, ochre or wood-colored or pale vinaceous buff when dry; pores angular isodiametric, and without tendency to become lamellate towards the margin, 3–4(–5) per mm; dissepiments thin, entire. Context concolorous with tube, extremely thin, up to 0.5 mm. Tubes gray to ochraceous or milky coffee, up to 7.5 mm long.

Hyphal structure – Hyphal system dimitic; generative hyphae with clamp connections, hyaline, thin-walled; skeletal hyphae distinctly thick-walled to subsolid, slightly dextrinoid, CB–; tissues darkening in KOH.

Context – Generative hyphae hyaline, thin-walled, occasionally branched, 2–3 μm in diam.; skeletal hyphae thick-walled with a narrow lumen to subsolid, unbranched, loosely interwoven, 2–7 μm in diam.

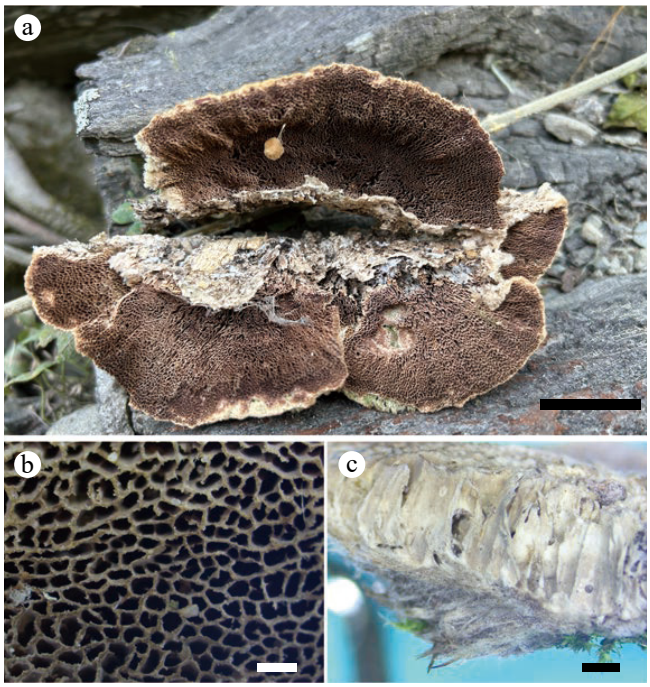

Fig. 11 Basidiomata of *Trichaptum longisporum* JV 2311/13-J (holotype). Scale bars: (a) = 1 cm, (b) and (c) = 1 mm.

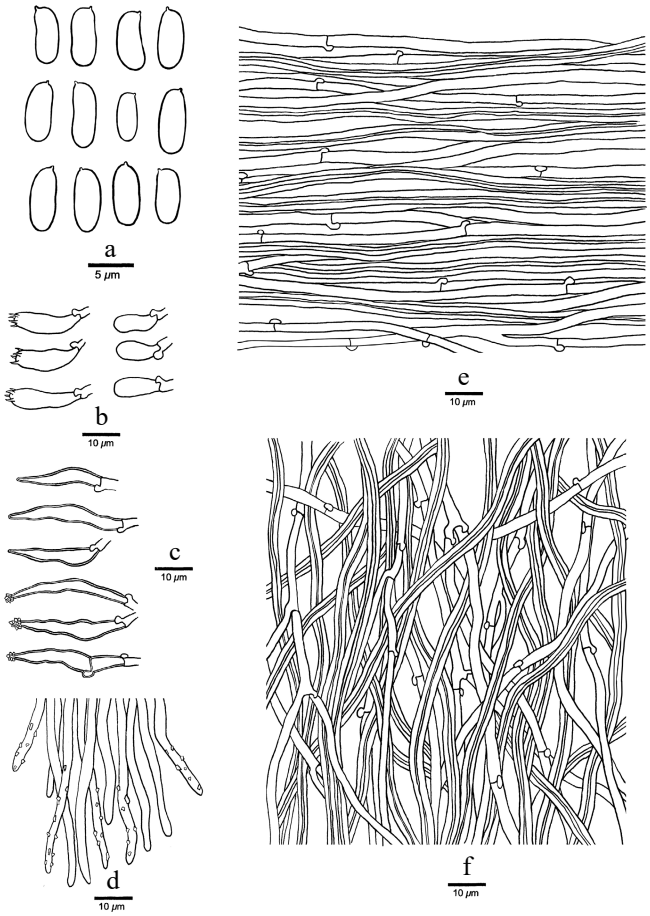

Fig. 12 Microscopic structures of *Trichaptum longisporum* (drawn from the holotype, JV 2311/13-J). (a) Basidiospores. (b) Basidia and basidioles. (c) Cystidia. (d) Hyphae at dissepiment edge. (e) Hyphae from context. (f) Hyphae from trama.

Tubes – Generative hyphae hyaline, thin-walled, usually branched, 2–2.5 μm in diam.; skeletal hyphae thick-walled with a wide lumen, unbranched, loosely interwoven to subparallel, 2–3 μm in diam.; hyphae at dissepiment loosely encrusted with small crystals.

Hymenium – Cystidia narrow fusoid to subulate, thin- to slightly thick-walled, mostly with long narrow necks up to 5–10 × 1.5 μm, apically encrusted, sometimes with several separate, 20–30 × 3–4 μm; hyphal pegs present; basidia barrel-shaped, with four sterigmata and a basal clamp connection, 16.5–22 × 5.5–7 μm; basidioles similar to basidia in shape, but smaller.

Spores – Basidiospores cylindrical to slightly allantoid, hyaline, thin-walled, smooth, IKI–, CB–, (6–)6.3–8(–8.4) × (2.5–)2.7–3.6(–3.8) μm, L = 7.20μm, W = 3.21 μm, Q = 2.13–2.35 (n = 60/3).

Type of rot – White rot.

Distribution and ecology – *Trichaptum longisporum* is a common species found in northeastern South America, growing on angiosperm trunks.

Specimens examined – BRAZIL. Piauí, Caracol, 2011, URM 83620 & B530 (URM 83620 & BJFC032949). BOLIVIA, St. Cruz Dept., Refugio los Volcanes, XI. 2023, JV 2311/13-J (holotype BJFC044759), JV 2311/18-J (BJFC044760), JV 2311/19-J (BJFC044761); COSTA RICA. Guanacaste Prov., Rincón de la Vieja Volcano, Guachipelin, on fallen log, 10.III. 2022, JV2203/72-J; on fallen branch of *Quercus*, 12.III. 2022, JV 2203/104 (BJFC044762); ECUADOR. Arenillas, 17.II.2024, JV 2402/9-J; JAMAICA. IX. 2008, JV 0809/19-J (BJFC032949).

Key to known species of Trichaptum

1.	Basidiomata usually resupinate	*T. resacarium*
1.	Basidiomata pileate to effused-reflexed	2
2.	Basidiosporesr < 4 μm in length	*T. resacarium*
2.	Basidiospores > 4 μm in length	*T. cystidiolatum*
3.	Pores round to angular, 6–7 per mm	*T. perpusillum*
3.	Pores angular to irpicoid, < 5 per mm	4
4.	Basidiospores > 4 μm in width	*T. anomalum*
4.	Basidiospores < 4 μm in width	5
5.	Pore surface snuff brown to cigar brown	*T. perrottetii*
5.	Pore surface light grayish brown to wood-colored or pale vinaceous buff	6
6.	Pores 3–5 per mm; basidiospores < 5.5 μm in length	*T. strigosum*
6.	Pores 0.5–3 per mm; basidiospores > 5.5 μm in length	7
7.	Pore surface vinaceous brown, basidiospores 2–2.5 μm in width	*T. byssogenum*
7.	Pore surface cream to wood-colored, basidiospores 2.7–3.6 μm in width	*T. longisporum*

Podocarpioporus hydnoides Meng Zhou, Y.J. Cui, H. Zhao, Y.C. Dai & Yuan Yuan, sp. nov. (Figs 13,14)

MycoBank number: MB 861994

Type – CHINA. Xizang Auto. Reg., Linzhi County, on fallen trunk of *Pinus yunnanensis*, 27, X, 2023 Dai 26968 (Holotype BJFC044520).

Etymology – *Hydnoides* (Lat.): refers to the species having a hydnoid hymenophore.

Basidiomata – Annual, resupinate, soft to soft leathery when fresh, becoming corky upon drying, up to 6 cm long, 4 cm wide, and 5 mm thick at the center. Hymenophore hydnoid, cream when fresh, buff to vinaceous brown when dry; teeth 4–6 per mm; dissepiments strongly lacerate. Context cream, up to 0.5 mm thick. Tubes pale brown, up to 1.5 mm long.

Hyphal structure – Hyphal system dimitic; generative hyphae with clamp connections, hyaline, thin-walled; skeletal hyphae distinctly thick-walled, slightly dextrinoid, CB+; tissues unchanged in KOH.

Context – Generative hyphae hyaline, thin- to thin-walled, unbranched, 1–2 μm in diam.; skeletal hyphae thick-walled with a narrow lumen, unbranched, interwoven, 1.5–3 μm in diam.

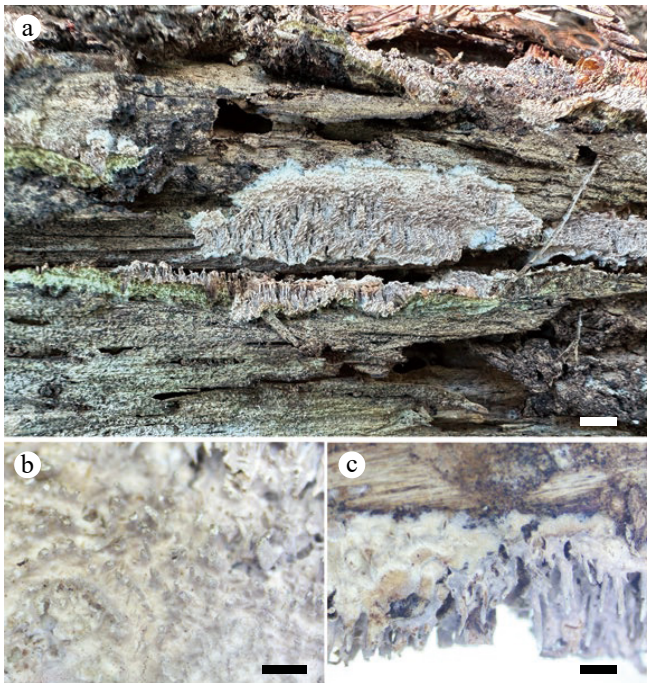

Fig. 13 Basidiomata of *Podocarpioporus hydnoides* Dai 26968. Scale bars: (a) = 1 cm, (b) and (c) = 1 mm.

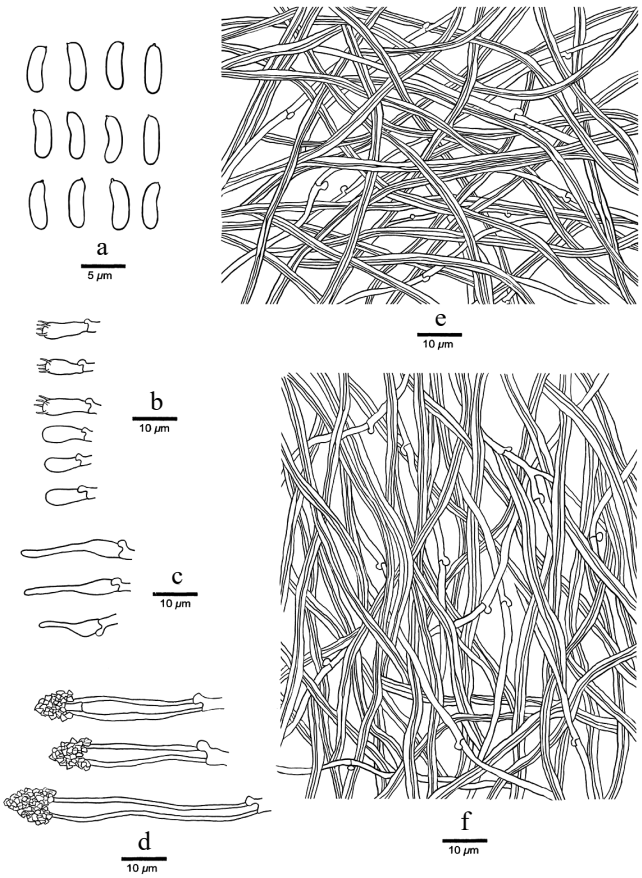

Fig. 14 Microscopic structures of *Podocarpioporus hydnoides* (Dai 26968). (a) Basidiospores. (b) Basidia and basidioles. (c), (d) Cystidia. (e) Hyphae from context. (f) Hyphae from trama.

Tubes – Generative hyphae hyaline, thin-walled, occasionally branched, 1–2.5 μm in diam.; skeletal hyphae thick-walled, unbranched, interwoven, 2–3.5 μm in diam.

Hymenium – Cystidia clavate to fusoid, thin-walled, abundant, hyaline, thick-walled, apically encrusted, 37–80 × 5–6.5 μm; cystidioles present, fusoid with a long neck, thin-walled, smooth, 12–25 × 3–4 μm; basidia clavate, with four sterigmata and a basal clamp connection, 11–16 × 3.5–4.5 μm; basidioles similar to basidia in shape, but smaller.

Spores – Basidiospores cylindric to slightly allantoid, hyaline, thin-walled, smooth, IKI–, CB–, (4.3–)4.7–6.5 × (1.2–)1.3–2.1(–2.2) μm, L = 5.78 μm, W = 1.78 μm, Q = 3.20–3.35 (n = 90/3).

Type of rot – White rot.

Distribution and ecology – *Podocarpioporus hydnoides* to date, is found only in Xizang Auto. Reg. CHINA.

Specimens examined – CHINA. Xizang Auto. Reg., Linzhi county, on fallen trunk of *Pinus yunnanensis*, 27, X, 2023, Dai 26909 (BJFC044460); Dai 26920 (BJFC044471); Dai 26968 (holotype BJFC044520); Dai 27008 (BJFC044560); Dai 27037 (BJFC044589); on charred wood of *Pinus yunnanensis*, Dai 26959 (BJFC044510).

Notes – *Podocarpioporus hydnoides* is characterized by narrow allantoid basidiospores, distinctly long subulate hymenial cystidia, which fit the definition of *Podocarpioporus*. Phylogenetically, four samples of *Podocarpioporus hydnoides* formed an independent lineage that is closely related to *P. podocarpi*. The latter differ from *P. hydnoides* in having a poroid to irpicoid hymenophore when juvenile and a lack of cystidioles.

Ancestral biogeography estimation

Dataset 3, comprising 52 specimens, was used to infer the historical biogeography and ancestral state of basidiomata of *Trichaptum* s.l. using RASP v.4.2[79,80] under the S-DEC and Bayesian Binary MCMC models. The biogeographical analyses indicated that *Trichaptum* s.l. has a complex evolutionary history, with its most recent common ancestor likely originating in Central and East Asia (Fig. 15, node 1). Throughout its evolutionary history, *Trichaptum* s.l. has experienced 49 global dispersal events, eight global vicariance events, one global extinction event, and 48 speciation events.

At the family level, Hirschioporaceae and Pseudotrichaptaceae are reconstructed with the highest probability as originating in Central and East Asian (Fig. 15, nodes 2 and 3), while the origin of Podocarpioporaceae (Fig. 15, node 4) remains ambiguous, with analyses showing comparable support for origins in Central and East Asia or South to Southeast Asia and Oceania. In contrast, Trichaptaceae appears to have an origin in Central and South America (Fig. 15, node 5).

At the genus level, *Pseudotrichaptum*, *Podocarpioporus*, and *Trichaptum* align with their respective families, as each corresponds to a monotypic family. The genera within Hirschioporaceae exhibit distinct biogeographical origins: *Hirschioporus* likely originated in North America (Fig. 15, node 6), *Perennihirschioporus* in South to Southeast Asia and Oceania (Fig. 15, node 7), *Nigrohirschioporus* shows a primary probability for a Central and South American origin (Fig. 15, node 8), alternative scenarios involving Central and East Asia cannot be ruled out. This uncertainty likely reflects the complex pantropical distribution of these lineages. Lastly, *Pallidohirschioporus* is inferred to have origins in regions excluding Africa (Fig. 15, node 9).

Climate distribution patterns estimation

A total of 44 global dispersal events and eight global vicariance events were inferred using RASP v.4.2[79,80] under the S-DEC and Bayesian Binary MCMC models. The most recent common ancestor of *Trichaptum* s.l. was likely distributed in tropical regions, with subsequent dispersal into subtropical, tropical, and mountain zones (Fig. 16 node 1). Hirschioporaceae is most likely of tropical origin (Fig. 16 node 2), while Pseudotrichaptaceae (with the single genus *Pseudotrichaptum*) is inferred to have originated in temperate to subtropical zones (Fig. 16 node 3). Both Podocarpioporaceae (with the single genus *Podocarpioporus*) and Trichaptaceae (with the single genus *Trichaptum*) are inferred to have originated in subtropical to tropical zones (Fig. 16 nodes 4 and 5). Within Hirschioporaceae, *Hirschioporus* likely originated in temperate zones (Fig. 16 node 6), while *Nigrohirschioporus* and *Perennihirschioporus* are inferred to have originated in tropical zones (Fig. 16 nodes 7 and 8). The origin of *Pallidohirschioporus* remains unresolved, with all climatic zones being equally plausible (Fig. 16 node 9).

Ancestral characters evolution

Ancestral character reconstruction was used to examine the evolutionary configuration of basidiomata in *Trichaptum* s.l. using RASP v.4.2[79,80] under the S-DEC and Bayesian Binary MCMC models. RASP analyses suggested that the ancestral morphology of *Trichaptum* s.l. most likely consisted of a coriaceous consistency with a tomentose surface or apileate (Fig. 17). However, node support values indicate some uncertainty at deeper nodes, suggesting that alternative ancestral states (e.g., soft corky consistency) are possible. Despite this ambiguity, a general trend toward increasing basidiomata hardness is observable throughout the evolutionary history of the group.

Regarding basidiomata consistency, the ancestral state of Hirschioporaceae was inferred to be either coriaceous or woody hard, whereas that of Pseudotrichaptaceae and Trichaptaceae was most likely coriaceous. The ancestral consistency of Podocarpioporaceae was inferred to be either soft corky (becoming brittle when dry) or coriaceous. Within Hirschioporaceae, the ancestral consistency was reconstructed as coriaceous for *Hirschioporus*, *Pallidohirschioporus*, and *Perennihirschioporus*, while for *Nigrohirschioporus* it was either woody hard or soft, corky to brittle when dry.

The ancestral surface morphology of the pileal surface in Hirschioporaceae was likely tomentose or warted. In Pseudotrichaptaceae and Podocarpioporaceae, the ancestral condition is inferred to be tomentose or apileate. Trichaptaceae likely originated with a hispid surface or was apileate. Within Hirschioporaceae, the ancestral morphology was reconstructed as tomentose for *Hirschioporus* and *Pallidohirschioporus*, warted or apileate for *Nigrohirschioporus*, and warted for *Perennihirschioporus*.

Species distribution of *Trichaptum* s.l. and environmental factors

To investigate the distribution patterns of each genus within the broad *Trichaptum* s.l., global occurrence data at the genus level were compiled and categorized, based on the revised taxonomic system of *Trichaptum* s.l. revised in this study (Fig. 18, Table 5). This dataset integrated both publicly available records and data from specimens examined herein. Subsequently, a comprehensive suite of environmental variables was screened to identify the primary climatic drivers for each genus. The objective was to determine the factors with the highest contribution rates in the models, through which the adaptive relationships between the fungal lineages and their climatic niches could be explored.

Genus Hirschioporus

The genus *Hirschioporus* exhibits a North Temperate distribution pattern, with its species primarily inhabiting coniferous wood

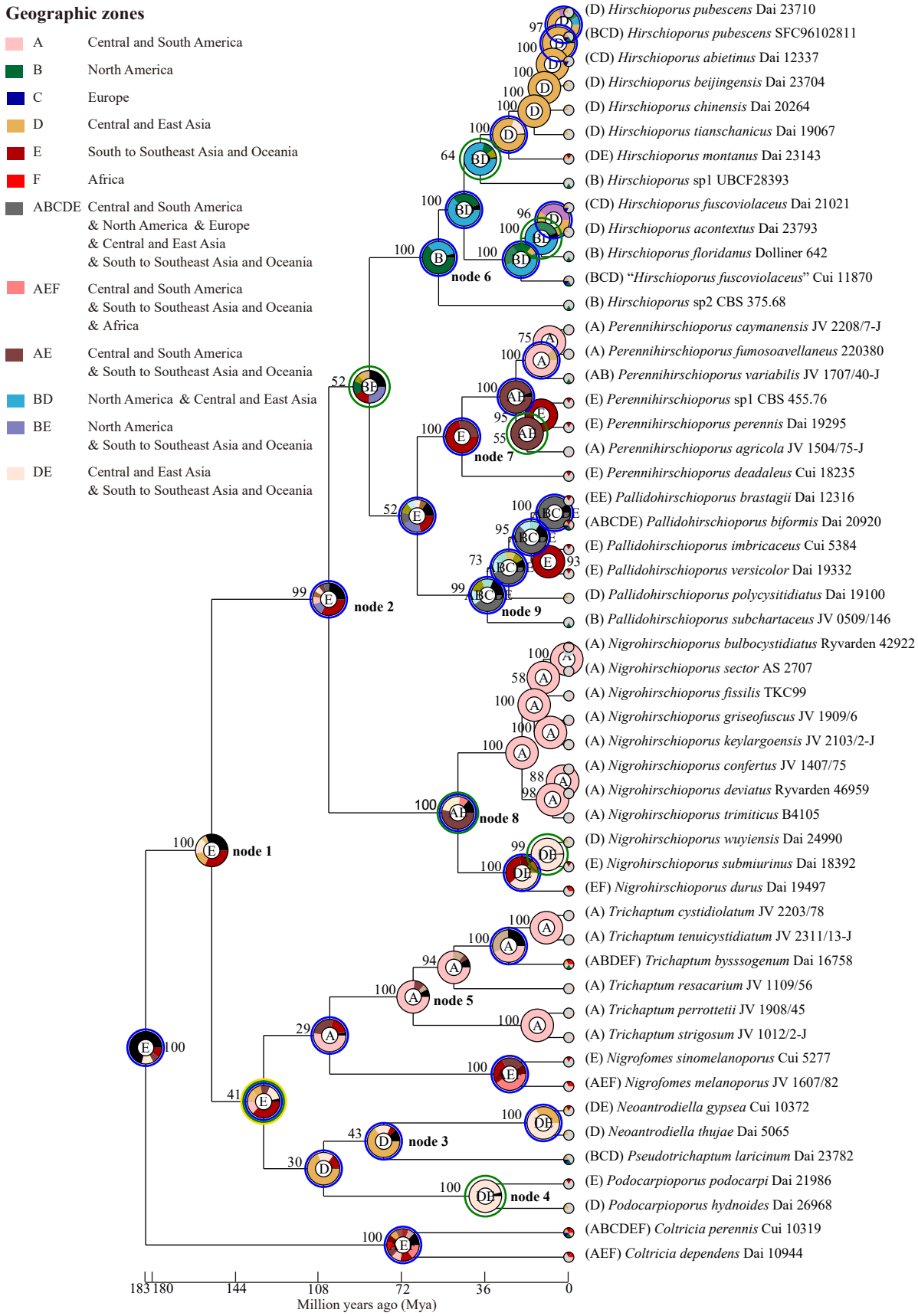

Fig. 15 The origin of geographical distribution of the *Trichaptum* s.l., A. Central and South America, B. North America, C. Europe, D. Central and East Asia, E. South to Southeast Asia and Oceania, and F. Africa. The phylogenetic tree was generated with Bayesian Inference algorithms using BEAST, while the trait of the pie chart at each node was evaluated using RASP under the Bayesian Binary MCMC model. The trait represented by each color and letter in the pie chart is indicated in the upper left with the supported values.

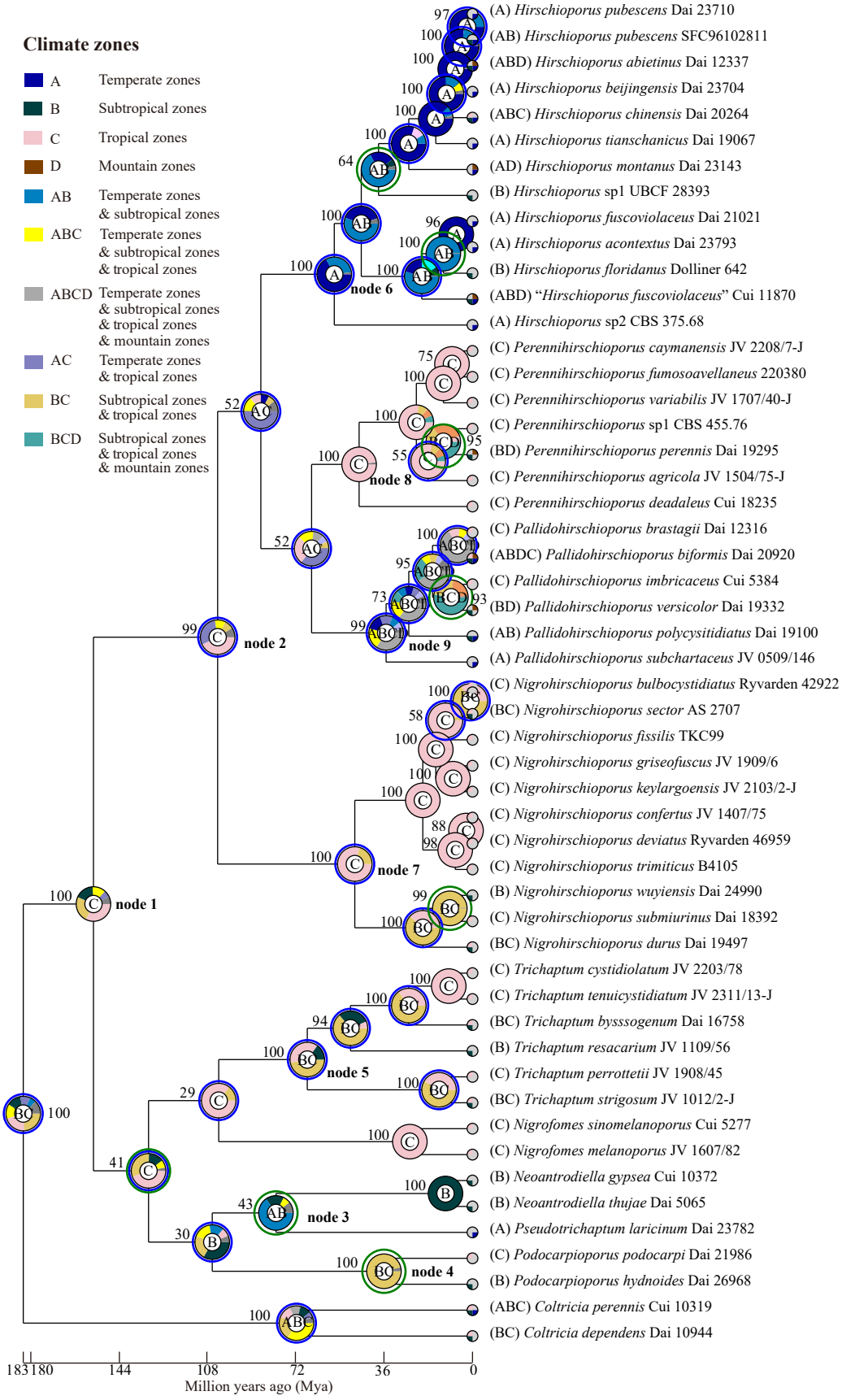

Fig. 16 The origin of climate distribution of the *Trichaptum* s.l., A. Temperate zones, B. Subtropical zones, C. Tropical zones, and D. Mountain zones. The phylogenetic tree was generated with Bayesian Inference algorithms using BEAST, while the trait of the pie chart at each node was evaluated using RASP under the Bayesian Binary MCMC model. The trait represented by each color and letter in the pie chart is indicated in the upper left with the supported values.

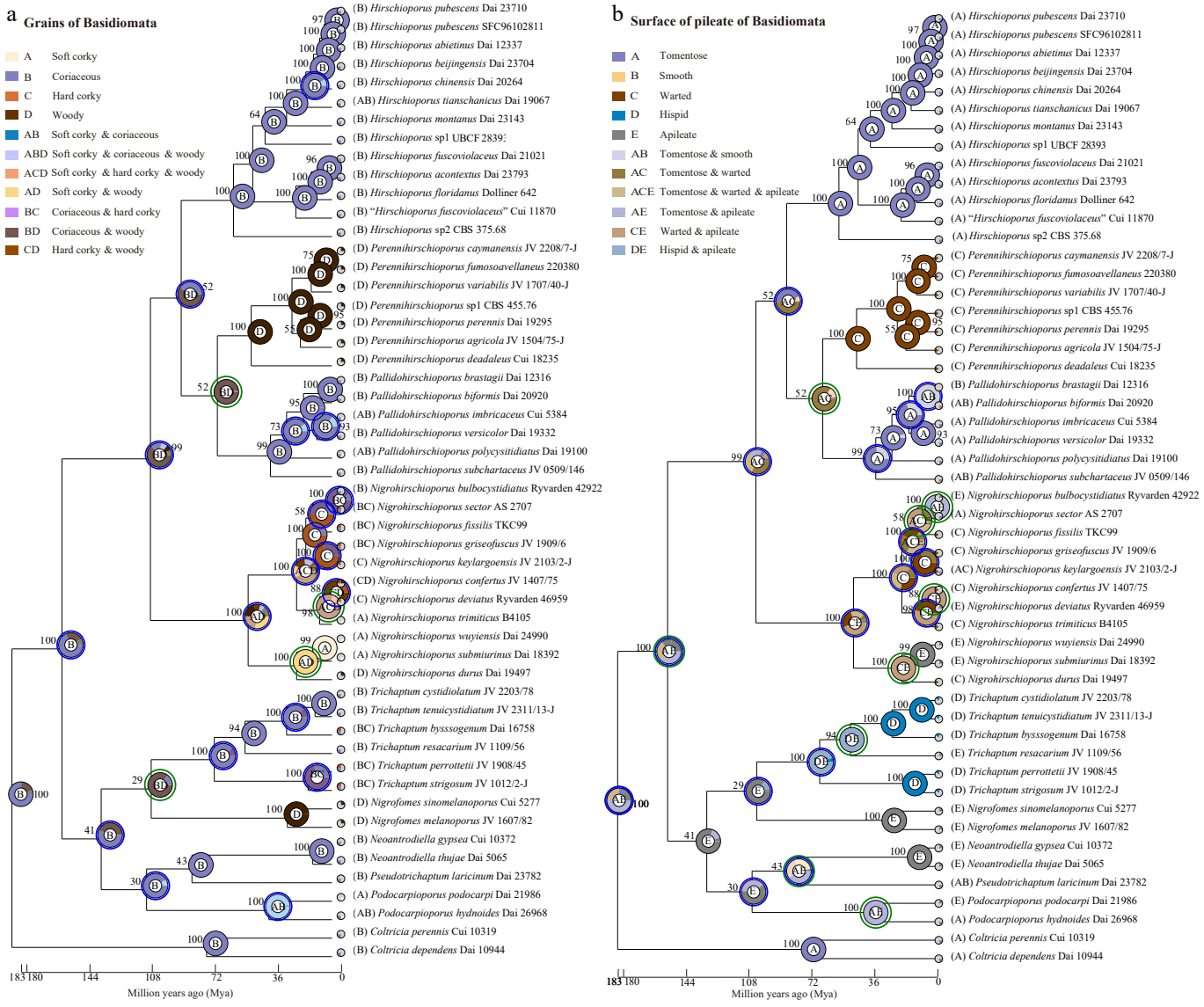

Fig. 17 The configuration evolution of basidiomata of *Trichaptum* s.l., (a) consistency and (b) surface of pileus. The phylogenetic tree was generated with Bayesian Inference algorithms using BEAST, while the trait of the pie chart at each node was evaluated using RASP under the Bayesian Binary MCMC model. The trait represented by each color and letter in the pie chart is indicated in the upper left with the supported values. Four types of consistency, A. Soft corky to brittle when dry, B. Coriaceous, C. Hard corky, and D. Woody hard. Five types of surfaces of pileate, A. Tomentose, B. Smooth, C. Warted, D. Hispid, and E. Apileate.

throughout Eurasia, North America, and the Himalayas. Species within this genus are typically saprophytic, functioning as pioneer decomposers that colonize dead trees and newly fallen logs.

The distribution of the genus is primarily concentrated in temperate and subtropical regions. However, influenced by geographical and historical factors, its range has expanded southward along mountain ranges to occupy alpine zones in the tropics and temperate regions of the Southern Hemisphere. Nevertheless, our ancestral biogeography analysis reveals that the ancestral origin and center of distribution for *Hirschioporus* remains in the North Temperate zone (Fig. 15). The hosts of *Hirschioporus* are exclusively gymnosperms, primarily pine (*Pinus* spp.), spruce *(Picea* spp.), fir (*Abies* spp.), and larch (*Larix* spp.). For the environmental niche analysis, we aggregated occurrence data from the GBIF and field specimens collected in this study. The initial dataset of 45,937 records was refined by removing duplicate entries and applying a spatial thinning filter with a 2.5 arc-min resolution. This process resulted in a final dataset of 36,607 unique occurrence points, which were used to model environmental factors. The global distribution of these points is mapped in Fig. 18a.

Table 5 presents the average relative contributions of the predictor variables from the Maxent model (i.e., those with a contribution > 5%, permutation importance > 5%). The species distribution model for the genus *Hirschioporus* achieved a fair predictive performance, with an average Area Under the Curve (AUC) value of 0.693 ± 0.003 across 15 replicate runs (Supplementary Fig. S1a). The analysis of variable contributions identified climatic factors related to summer thermal stress and annual moisture availability as the primary drivers of the genus's distribution (Table 5). According to the permutation importance metric, the maximum temperature of the warmest month (Bio5) was the most critical limiting factor, contributing 29.3% to the model's predictive power. The second most important variable was annual precipitation (Bio12), with a permutation importance of 18.3%. While precipitation of the driest month (Bio14) showed the highest percent contribution (51.1%), its negligible permutation importance (0.8%) suggests its influence is

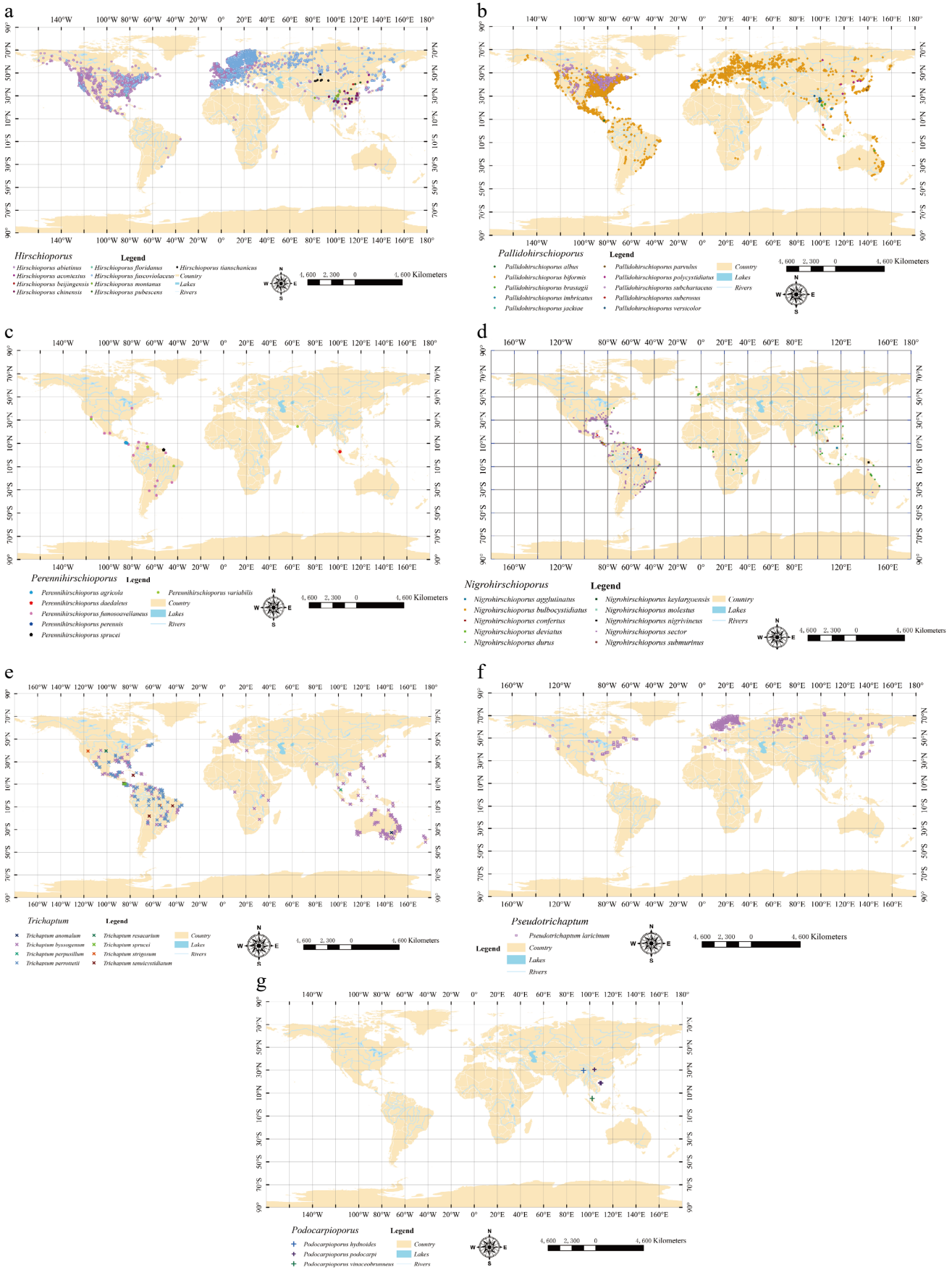

Fig. 18 Global distribution map of *Trichaptum* s.l. genera based on spatially thinned and verified GBIF occurrence records. (a) *Hirschioporus*, (b) *Pallidohirschioporus*, (c) *Perennihirschioporus*, (d) *Nigrohirschioporus*, (e) *Trichaptum*, (f) *Pseudotrichaptum*, and (g) *Podocarpioporus*. Source: World Map (1:10,000,000), the Natural Earth website, www.naturalearthdata.com.

likely an artifact of its correlation with other more causally-related variables. The response curves for the key environmental variables further defined the ecological niche of *Hirschioporus* (Supplementary Fig. S1). The genus exhibited a clear intolerance to high summer heat, with habitat suitability peaking where the maximum temperature of the warmest month (Bio5) was between 20–25°C, and declining sharply thereafter (Supplementary Fig. S1b). The model also demonstrated a strong positive response to moisture, with suitability increasing steadily with annual precipitation (Bio12) (Supplementary Fig. S1c). The Jackknife test indicates that annual mean temperature (Bio1) is the variable with the greatest amount of information when used alone (Supplementary Fig. S1e). The response toBio1 showed a broad optimum centered around 0–15°C, consistent with adaptation to temperate climates (Supplementary Fig. S1d).

Genus Pallidohirschioporus

The genus *Pallidohirschioporus* is widely distributed across temperate and subtropical regions worldwide, with documented occurrences in North America, Europe, Asia, and Australia. It primarily exhibits a temperate to subtropical distribution pattern. While individual species within the genus show varied host and climatic preferences, the majority are found on angiosperm wood, including oak (*Quercus* spp.), birch (*Betula* spp.), poplar (*Populus* spp.), and plum (*Prunus* spp.). The main distribution pattern is exemplified by temperate-subtropical species such as *P. biformis*, *P. jackiae*, *P. parvulus*, *P. polycystidiatus*, *P. subchartaceus*, and *P. versicolor*. However, a subset of species, including *P. albus*, *P. brastagii*, *P. imbricatus*, and *P. suberosus*, is distributed in tropical regions.

Table 5. Contribution of various environmental variables to the distribution of *Trichaptum* s.l.

Genera	Abbreviation	Environmental factors	Units	Rate of contribution (%)	Permutation importance (%)
Hirschioporus	Bio14	Precipitation of driest month	mm	51.1	0.8
	Bio12	Annual precipitation	mm	23.4	18.3
	Bio1	Annual mean temperature		6	4.6
	Bio11	Mean temperature of coldest quarter	°C	6	1
	Bio6	Maximum temperature of warmest month	°C	3.8	7.8
	Bio5	Maximum temperature of warmest month	°C	2.9	29.3
	Bio7	Temperature annual range (Bio5-Bio6)	°C	1.9	5.7
	Bio19	Precipitation of coldest quarter	mm	0.9	8.7
	Bio10	Mean temperature of warmest quarter	°C	1.2	8.5
	Bio16	Precipitation of wettest quarter	mm	0.3	5.3
Pallidohirschioporus	Bio14	Precipitation of driest month	mm	41.5	0.7
	Bio12	Annual precipitation	mm	22	5.2
	Bio17	Annual mean temperature	mm	11.3	13.6
	Bio 5	Maximum temperature of warmest month	°C	7.8	25.5
	Bio11	Mean temperature of coldest quarter	°C	7.5	10.1
	Bio10	Mean temperature of warmest quarter	°C	0.9	18.4
	Bio16	Precipitation of wettest quarter	mm	0.5	9.2
	Bio19	Precipitation of coldest quarter	mm	0.4	7.4
Perennihirschioporus	Bio16	Precipitation of wettest quarter	mm	58.7	3.9
	Bio3	Isothermality (Bio2/Bio7) (× 100)	C of V	10.8	10.3
	Bio4	Temperature seasonality (standard deviation x 100)	°C	7.1	2.3
	Bio18	Precipitation of warmest quarter	mm	2.6	5.4
	Bio19	Precipitation of coldest quarter	mm	4.8	12.5
	Bio7	Temperature annual range (Bio5-Bio6)	°C	1	10.7
	Bio8	Mean temperature of wettest quarter	°C	0.7	14.6
	Bio9	Mean temperature of driest quarter	°C	0.4	10.7
Nigrohirschioporus	Bio12	Annual precipitation	mm	61.3	5.8
	Bio3	Isothermality (Bio2/Bio7) (× 100)	C of V	13.3	10.7
	Bio11	Mean temperature of coldest quarter	°C	6.9	46.3
	Bio14	Precipitation of driest month	mm	6.6	5.8
	Bio4	Temperature seasonality (standard deviation x 100)	°C	1.2	5.2
Trichaptum s.s.	Bio6	Minimum temperature of coldest month	°C	20.1	0.1
	Bio12	Annual precipitation	mm	20.1	11.2
	Bio14	Precipitation of driest month	mm	15.3	4.5
	Bio3	Isothermality (Bio2/Bio7) (× 100)	C of V	12	8.2
	Bio19	Precipitation of coldest quarter	mm	7.7	4.2
	Bio4	Temperature seasonality (standard deviation x 100)	°C	4.7	10
	Bio18	Precipitation of warmest quarter	mm	3.5	8.8
	Bio7	Temperature annual range (Bio5-Bio6)	°C	2.3	5.3
	Bio13	Precipitation of wettest month	mm	0.8	5.6
Pseudotrichaptum	Bio14	Precipitation of driest month	mm	57.6	1.1
	Bio1	Annual mean temperature	°C	17.2	8.9
	Bio5	Max temperature of warmest month	°C	7.7	42.3
	Bio18	Precipitation of warmest quarter	mm	4.1%	6
	Bio4	Temperature seasonality (standard deviation x 100)	C of V	2.5%	15.1
	Bio8	Mean temperature of wettest quarter	°C	1.2	6.3
	Bio20	Elevation	mm	0.7	8.8
	Bio10	Mean temperature of warmest quarter	°C	0.5	5.9

According to GBIF records and field data from specimens collected for this study, there was a total of 53,793 valid occurrence records for *Pallidohirschioporus* species. After removing duplicates and overlapping points within a 2.5 arc-minute resolution, 10,393 occurrence points were retained to screen for the primary environmental factors influencing this fungal genus. Its global distribution map is shown in Fig. 18b. The Maxent model developed for *Pallidohirschioporus* demonstrated good predictive accuracy, achieving an average test AUC of 0.788 ± 0.004. The analysis of environmental variable contributions identified a combination of seasonal temperature and precipitation factors as primary drivers. According to permutation importance, the most influential variables were the maximum temperature of the warmest month (Bio5; 25.5%), the mean temperature of the warmest quarter (Bio10; 18.4%), the precipitation of the driest quarter (Bio17; 13.6%), and the mean temperature of the coldest quarter (Bio11; 10.1%) (Table 5).

Response curves revealed that the genus thrives in warm conditions, with habitat suitability peaking when the maximum temperature of the warmest month (Bio5) is approximately 30 °C (Supplementary Fig. S2c). The genus also requires moisture, showing a strong positive response to annual precipitation (Bio12) and a preference for regions where the precipitation of the driest quarter (Bio17) remains above a minimum threshold (Supplementary Fig. S2b, S2d). Furthermore, its distribution is limited by cold winters, as suitability drops sharply when the mean temperature of the coldest quarter (Bio11) falls below 0 °C (Supplementary Fig. S2e).

Genus Perennihirschioporus

The genus *Perennihirschioporus* is distributed in tropical and subtropical regions, primarily within semi-arid climate zones. The genus exhibits a tropical Asian-American disjunct distribution pattern, meaning its species are found in the warm regions of Asia and the Americas, but not in the intervening areas. In the Eastern Hemisphere, its range may extend from Asia to northeastern Australia and potentially to the islands of the southwestern Pacific. Species of *Perennihirschioporus* grow on various angiosperm wood. According to GBIF records and field data from specimens collected for this study, there was a total of 70 valid occurrence records for *Perennihirschioporus* species. After removing duplicates and overlapping points within a 2.5 arc-min resolution, 43 occurrence points were retained to screen for the primary environmental factors influencing this fungal genus. Its global distribution map is shown in Fig. 18c.

The Maxent species distribution model for *Perennihirschioporus* achieved excellent predictive accuracy, with an average test AUC of 0.924 ± 0.020. The high performance of the model suggests a highly specialized and narrowly defined climatic niche for the genus. The analysis of environmental variable contributions revealed that precipitation of the wettest quarter (Bio16) was the overwhelmingly dominant factor driving the distribution, accounting for 58.7% of the model's predictive power (Table 5). The next most important variables, isothermality (Bio3; 10.8%) and temperature seasonality (Bio4; 7.1%), also point to the importance of a stable tropical climate. The critical role of Bio16 was further confirmed by the Jackknife test, which showed it possessed the highest gain when used in isolation by a large margin (Supplementary Fig. S3). Response curves indicated that the habitat suitability of *Perennihirschioporus* increases dramatically with precipitation of the wettest quarter (Bio16), peaking in regions that receive 1,000–2,000 mm of rain during the wet season (Supplementary Fig. S3b). The genus also showed a clear preference for areas with high isothermality (Bio3) and low temperature seasonality (Bio4), characteristics of climates with minimal temperature fluctuation (Supplementary Fig. S3c, S4d).

Genus Nigrohirschioporus

The genus *Nigrohirschioporus*, a group of poroid fungi colonizing angiosperm wood, exhibits a classic pantropical rainforest distribution pattern, which was concentrated in the world's three major tropical rainforest basins: the Amazon Basin in South America, the Congo Basin in Africa, and the Malesian region in Southeast Asia.

According to GBIF records and field data from specimens collected for this study, there was a total of 628 valid occurrence records for *Nigrohirschioporus* species. After removing duplicates and overlapping points within a 2.5 arc-min resolution, 510 occurrence points were retained to screen for the primary environmental factors influencing this fungal genus. Its global distribution map is shown in Fig. 18d. The Maxent model for the genus *Nigrohirschioporus* achieved excellent predictive accuracy, with a high average test AUC of 0.954 ± 0.004. This result indicates a well-defined and highly specialized climatic niche. The analysis of variable importance identified the mean temperature of the coldest quarter (Bio11) as the primary limiting factor for the genus's distribution. It had the highest permutation importance by a large margin, at 46.3% (Table 5). While annual precipitation (Bio12) had the highest percent contribution (61.3%), its lower permutation importance (5.8%) suggests it is a necessary but less critical limiting factor at the global scale compared to thermal constraints. Response curves illustrated the genus's strict climatic requirements (Supplementary Fig. S4). Habitat suitability was highest where the mean temperature of the coldest quarter (Bio11) remained above 18 °C, dropping precipitously at lower temperatures (Supplementary Fig. S4b). The genus also showed a strong positive response to high annual precipitation (Bio12) and high isothermality (Bio3), underscoring its adaptation to stable, consistently warm, and humid environments (Supplementary Fig. S4c, S4d).

Genus Trichaptum s.s.

The genus *Trichaptum* exhibits a pantropical distribution pattern, with a majority of its species occurring in tropical and subtropical regions. Ecologically, it is primarily found on angiosperm wood. According to GBIF records and field data from specimens collected for this study, there was a total of 555 valid occurrence records for *Trichaptum* s.s. species. After removing duplicates and overlapping points within a 2.5 arc-min resolution, 554 occurrence points were retained to screen for the primary environmental factors influencing this fungal genus. Its global distribution map is shown in Fig. 18e.

The Maxent model for the genus *Trichaptum* achieved excellent predictive accuracy, with a high average test AUC of 0.941 ± 0.006. This result indicates a well-defined and highly specialized climatic niche for the genus. The analysis of variable contributions identified a combination of thermal limits and moisture availability as the primary drivers of distribution. Minimum temperature of coldest month (Bio6) and annual precipitation (Bio12) showed the highest percent contributions (both 20.1%). However, permutation importance analysis highlighted the mean temperature of the warmest quarter (Bio10) as the most critical variable (18.0% importance), followed by annual precipitation (Bio12, 11.2%) (Table 5). Response curves illustrated the genus's strict climatic requirements (Supplementary Fig. S5). Habitat suitability was strongly limited by winter cold, dropping to near zero when the minimum temperature of the coldest month (Bio6) fell below freezing (Supplementary Fig. S5b). The genus also requires high moisture, with suitability increasing with annual precipitation (Bio12) (Supplementary Fig. S5c). Furthermore, *Trichaptum* thrives in warm climates, showing a clear preference for areas where the mean temperature of the warmest quarter (Bio10) exceeds 25 °C (Supplementary Fig. S5d).

Genus Pseudotrichaptum

The genus *Pseudotrichaptum* comprises species that primarily inhabit coniferous trees. It exhibits a circumboreal distribution, with species widely distributed throughout the coniferous forests of the Northern Hemisphere. These fungi demonstrate low host specificity, capable of colonizing the wood of fir (*Abies*), larch (*Larix*), spruce (*Picea*), and pine (*Pinus*). According to GBIF records and field data from specimens collected for this study, there was a total of 6,242 valid occurrence records for *Pseudotrichaptum* species. After removing duplicates and overlapping points within a 2.5 arc-min resolution, 4,764 occurrence points were retained to screen for the primary environmental factors influencing this fungal genus. Its global distribution map is shown in Fig. 18f.

For our model, the mean value of the average AUC for the training set is 0.892 with a low standard deviation of 0.002, which indicated favorable model performance. The average relative contributions of the predictor variables from the Maxent model (more than 5%) are presented in. The analysis of variable importance identified temperature as the primary driver of the genus's distribution. According to permutation importance, the most critical variables were the maximum temperature of the warmest month (Bio5; 42.3% importance) and temperature seasonality (Bio4; 15.1%). Elevation also emerged as a significant factor (8.8% importance) (Table 5). Response curves illustrated the species' adaptation to cold climates (Supplementary Fig. S6). Habitat suitability peaked at an annual mean temperature (Bio1) near 0 °C (Supplementary Fig. S6b). The species demonstrated a strong intolerance to heat, with suitability dropping sharply when the maximum temperature of the warmest month (Bio5) exceeded 20 °C (Supplementary Fig. S6c). This thermal limitation defines its southern distribution boundary. Furthermore, its habitat suitability showed a positive correlation with elevation (Supplementary Fig. S6d), confirming its preference for high-altitude environments.

Genus Podocarpioporus

Podocarpioporus grows on the wood of *Dacrydium*, a genus within the Podocarpaceae family. The Podocarpaceae family itself is distributed in tropical and subtropical regions, with genera such as *Dacrydium* being sources of high-quality timber. *Podocarpioporus* exhibits a remarkable host specificity, growing exclusively on members of the Podocarpaceae, which strictly limits the dispersal. The primary host genus, *Dacrydium*, is mainly distributed in the mountainous regions of central and southern Hainan, China, as well as in Malaysia, Vietnam, Laos, Cambodia, Myanmar, and Thailand.

Discussion

Taxonomic implications and species diversity

Trichaptum s.l. was established in 1904, belonging to Hymenochaetales of Agaricomycetes within Basidiomycota, but its family-level classification has been controversial, and it has been considered a genus as incertae sedis[81–86]. The establishment of *Trichaptum* s.l. as a complex comprising two families and seven genera resolved long-standing taxonomic uncertainties[39]. The family Hirschioporaceae consisted of four genera, including *Hirschioporus*, *Nigrohirschioporus*, *Pallidohirschioporus*, and *Perennihirschioporus*, and Trichaptaceae included a single genus *Trichaptum*. However, previous studies focused on Asia, and the two genera *Podocarpioporus* and *Pseudotrichaptum* have not clearly defined their family-level taxonomic status.

In this study, four new species, *Nigrohirschioporus keylargoensis*, *Perennihirschioporus caymanensis*, *Trichaptum cystidiolatum*, and *T. longisporum*, collected from the subtropical to tropical North and South America, are described, greatly enriching the species diversity of *Trichaptum* s.l. in these regions. Additionally, two new species, *Nigrohirschioporus wuyiensis* and *Podocarpioporus hydnoides* are reported from temperate and subtropical China. The discovery of six new species from the Americas and Asia—supported by distinct molecular and morphological evidence—underscores the underestimated diversity of this group in tropical and subtropical regions.

Hirschioporaceae

In the phylogenetic analyses, two samples of *Nigrohirschioporus keylargoensis* formed a highly supported lineage (99/MP, 1/BI), which is sister to *N. griseofuscus*, and closely related to *N. fissilis* and *N. sector*. However, *N. griseofuscus* differs from *N. keylargoensis* in having a dimitic hyphal system and narrower basidiospores (Q = 3.17–3.30 vs. Q = 2.03–2.95). Both *N. fissilis* and *N. sector* differ from *N. keylargoensis* in having a regularly poroid hymenophore and a dimitic hyphal system. Morphologically, *Nigrohirschioporus keylargoensis* may be confused with *N. molestus* with hydnoid to irpicoid hymenophore and trimitic hyphal system; however, *N. molestus* is distinguished from *N. keylargoensis* by having smaller pores (3–4 per mm vs 1–2 per mm) and shorter ellipsoid basidiospores (4–4.8 × 3–3.5 μm vs 5.1–7.0 × 2–3 μm).

Nigrohirschioporus wuyiensis is recovered as an independent lineage sister to *N. submurinus*. Morphologically, *Nigrohirschioporus wuyiensis* may also be confused with *N. submurinus* and *N. deviatus* in its completely resupinate basidiomata and small pores. However, *N. submurinus* differs from *N. wuyiensis* in having smaller pores (6–9 per mm vs 4–6 per mm) and smooth fusoid cystidia with a long neck. *N. deviatus* is distinguished from *N. wuyiensis* by its narrow basidiospores (< 2μm in width vs > 2μm in width) and its angular or even split pore surface with poroid to irpicoid hymenophore.

Phylogenetically, *Perennihirschioporus caymanensis* forms an independent lineage that is related to *P. agricola*, *P. fumosoavellaneus*, and *P. variabilis*. *Perennihirschioporus variabilis* was originally described from Venezuela[87], and later found in French Guiana (JV1909/4-J). It has sometimes similar pilei as *P. caymanensis*, with poroid, irpicoid to daedaleoid hymenophore, but never lamellate, and basidiospores are bigger in *P. variabilis* than in *P. caymanensis* (4.5–6 × 2.2–2.5 μm vs 3.5–4.3 × 2–2.7 μm). *Perennihirschioporus agricola, P. fumosoavellaneus* have poroid hymenophores that are readily distinguished from *P. caymanensis*. *P. daedaleus* may also be confused with *P. caymanensis* in its perennial, pileate hymenophores. However, *P. daedaleus* is distantly related to *P. caymanensis* phylogenetically and is only found in Malaysia, which is far away from *P. caymanensis* geographically. Morphologically, *P. daedaleus* differs from *P. caymanensis* in having typically triquetrous basidiomata, with daedaleoid to hydnoid hymenophore and thinner context (0.1 mm vs 4 mm).

Trichaptaceae

In the phylogenetic analyses, three sequenced samples of *Trichaptum cystidiolatum* formed an independent lineage, closely related to *T. byssogenum* and *T. longisporum*. The latter two species differ from *T. cystidiolatum* in having distinctly pileate basidiomata. In addition, *T. longisporum* differs from *T. cystidiolatum* by smaller pores (3–4 per mm vs 1–3 per mm) and larger basidiospores (6.3–8 × 2.7–3.6 μm vs 4.5–6 × 2.2–2.9 μm). Morphologically, *T. cystidiolatum* and *T. resacarium* share similar resupinate to effused-reflexed basidiomata. However, *T. resacarium* is distinct by dark, greyish colors and smaller basidiospores (3.5–4 × 2 μm vs 4.5–6 × 2.2–2.9 μm).

Trichaptum cystidiolatum is so far only found in Costa Rica, but the same sequence, however, is present several times in GenBank as 'Uncultured fungus' (see Discussion). Ryvarden & Johansen[81] show a picture of *Trametes versatilis* Berk 1842 features (synonym of *Trichaptum byssogenum*, collected in the USA), where the spores correspond perfectly to our *T. cystidiolatum* spores. We have not seen its type in Kew, and so we cannot decide now if our *T. cystidiolatum* is identical with *Trametes versatilis* or not.

Phylogenetically, five samples of *Trichaptum longisporum* formed an independent lineage, which is closely related to *T. cystidiolatum* and *T. byssogenum*. Morphologically, *T. byssogenum* has a vinaceous brown pore surface and narrower basidiospores (2–2.5 μm in width vs 2.7–3.6μm in width) that can be distinguished from *T. longisporum*. Both *Funalia bouei* and *Polystictus hariotianus* are synonyms of *T. byssogenum* from South America, which has large pores (2 per mm) in the original description and is distinctly different from the small pores (3–4 per mm) of *T. longisporum*. *T. cystidiolatum* differs from *T. longisporum* by its effused-reflexed or resupinate basidiomata, larger pores (1–3 per mm vs 3–4 per mm), and smaller basidiospores (4.5–6 × 2.2–2.9 μm vs 6.3–8 × 2.7–3.6 μm).

Podocarpioporaceae

Podocarpioporus hydnoides is characterized by narrow allantoid basidiospores, distinctly long subulate hymenial cystidia, which fit the definition of *Podocarpioporus*. Phylogenetically, four samples of *Podocarpioporus hydnoides* formed an independent lineage that is closely related to *P. podocarpi*. The latter differ from *P. hydnoides* in having a poroid to irpicoid hymenophore when juvenile and a lack of cystidioles.

Evolutionary timeline and biogeographical history

Estimating the divergence times of Trichaptum s.l.

Currently, phylogenetic and morphological analyses are the main criteria for fungal species identification, and clock-dating analysis has gradually become a key basis for defining higher taxonomic units in fungi due to its important role in inferring fungal divergence times[17–19,21]. For example, He et al.[19] suggested that the divergence times within the phylum Basidiomycota for subphyla, classes, orders, and families are estimated to be 443–490 Mya, 312–412 Mya, 102–361 Mya, and 50–289 Mya, respectively. In recent years, the estimated divergence time of the order Hymenochaetales has been showed to range from 167 to 289 Mya[17,35,39,88]. Varga et al.[17] suggests that the rapid radiation of the orders within the class Agaricomycetes occurred during the Jurassic period. Additionally, Zhao et al. estimated that the divergence time of families within Hymenochaetales occurred between 123 and 163 Mya, corresponding to the Early Cretaceous to Late Jurassic periods[35]. These studies laid the foundation for estimating the divergence times of *Trichaptum* s.l. Zhou et al. estimated the mean stem ages of the families Hirschioporaceae and Trichaptaceae as 121 Mya and 103 Mya[39], respectively, which is in agreement with the results of this study. The mean stem ages of the four families within *Trichaptum* s.l. ranged from 71 Mya to 116 Mya, overlapping with results from previous studies[19,35,39,88] and supporting the legitimacy of the two newly proposed families. Meanwhile, the families in *Trichaptum* s.l. occurred during the Cretaceous, whereas individual species originated mainly during the Eocene to the Pleistocene, a period when the present-day continental configuration had largely taken shape. During this time, the global climate was warm and humid, and the diversity of both gymnosperms and angiosperms increased, providing favorable climatic conditions and abundant host trees that facilitated the rapid diversification of macrofungi[17,21,35,89–92].

The integration of divergence time estimates with biogeography and morphology represents an important approach for reconstructing the origin and evolution of macrofungi, as demonstrated in previous studies[17,21,35]. The centers of origin of macrofungi appear to be complex, with some lineages likely originating in Eurasia, such as *Onnia*, *Phaeolus*, *Porodaedalea*, and *Heterobasidion*, while others may have originated in Africa or the Americas, such as ectomycorrhizal Russulaceae and Hirschioporaceae[21,32,35,93–95]. In this study, the biogeographic reconstruction of *Trichaptum* s.l. revealed complex paleogeographic processes. Early divergences around 100–120 Mya coincide with the fragmentation of Gondwana, supporting possible African or South American origins for lineages such as Trichaptaceae[96]. In contrast, the wide distribution of Hirschioporaceae across the Northern Hemisphere may be associated with Laurasian connections and intercontinental dispersals facilitated by land bridges such as Beringia or the North Atlantic Land Bridge. This pattern has also been inferred for other macrofungi[16,33,97–99]. These patterns highlight the interplay between continental drift and fungal evolution. In addition, *Trichaptum* s.l. species distributed in the mountain zones of Central and East Asia exhibit relatively recent divergence times, later than 24 Mya (Figs 2, 15, and 16), and the uplift of the Xizang Plateau may have played an important role in their speciation[100].

Biogeographical history

Climatic adaptations further supported fungal evolutionary scenarios; some fungal groups may have originated in the tropical zone, such as ectomycorrhizal Russulaceae, and some possibly in the temperate zone, such as Hymenochaetales[21,35,92,99]. While *Trichaptum* s.l. species had a wide range of climate zones, from tropical to temperate, and mountain zones. Temperate-adapted clades from *Hirschioporus* and *Pallidohirschioporus* may have expanded during global cooling events of the Eocene–Oligocene transition (about 34 Mya), when temperate forests became widespread in the Northern Hemisphere[101].

With the *Trichaptum* s.l. species expanding from tropical zones to other climatic zones, their basidiomata gradually became more hardened. The coriaceous consistency evolved toward harder forms, including hard corky and woody hard, and the tomentose surface evolved into more specialized forms including smooth, warted, and hispid. The ancestral morphologies suggest a transition from softer to harder basidiomata, indicating an evolutionary trend towards increased structural rigidity. The convergence of similar traits across different clades inhabiting similar climates, such as woody basidiomata in both *Hirschioporus* (temperate) and *Perennihirschioporus* (tropical and mountain zones), suggest instances of parallel adaptation. These patterns likely reflect selection pressures shaped by macroecological factors[102], reinforcing the notion that basidiomata structure is not merely a taxonomic character but an adaptive trait molded by climate and substrate availability over evolutionary timescales. Additionally, similar to other groups of macrofungi, the morphological diversity of basidiomata may also contribute to the species diversity of *Trichaptum* s.l.[103]. Moreover, some *Trichaptum* s.l. species exhibit both extremely distant phylogenetic relationships and wide geographic separation, such as *Perennihirschioporus caymanensis* and *P. daedaleus*, yet share highly similar morphological characteristics that may be attributed to convergent evolution or atavistic evolution of different species under similar environmental conditions.

Adaptive radiation and ecological divergence

This study reveals three profoundly different climatic adaptation strategies among the three fungal families. The Hirschioporaceae

exemplifies a classic adaptive radiation across various climate zones. In contrast, the warm-temperate Trichaptaceae and the boreal-alpine Pseudotrichaptaceae each exhibit unique and fundamentally distinct ecological strategies.

Family Hirschioporaceae: a case study in adaptive radiation

The family Hirschioporaceae exhibits the most remarkable ecological plasticity, showing a clear evolutionary transition from tropical origins to boreal colonization through its four constituent genera, with a clear pattern of adaptive radiation from tropical to temperate and boreal zones.

Firstly, *Nigrohirschioporus* represents the ancestral ecological state, exhibiting strong niche conservatism. (Fig. 16). It is strictly confined to pantropical rainforests, governed by a 'thermal floor' (Bio11 > 18°C) and high year-round humidity. It lacks the physiological plasticity to tolerate cold or drought, effectively trapping it in stable, aseasonal tropical environments. This 'thermal floor' acts as a powerful biogeographical filter, strictly preventing its dispersal into subtropical or montane regions, even those that are sufficiently wet. Therefore, the distribution of *Nigrohirschioporus* is a classic example of a species whose range is defined not by the search for a resource (like water), but by the avoidance of a physiological stressor (cold). The strict adherence to a thermally stable, 'aseasonal' tropical niche. also confirms that *Nigrohirschioporus* has a long evolutionary history deeply rooted within these rainforest environments. Notably, *Nigrohirschioporus* is primarily distributed in the tropical regions of Southeast Asia and South America. It is considered an ecologically conservative lineage within the family, preserving ancestral ecological niches and distribution patterns. The discovery of *Nigrohirschioporus wuyiensis* in this study, a rare subtropical species within the genus, provides robust evidence for an evolutionary trend involving the gradual expansion of this genus towards subtropical zones.

This study provides strong quantitative support for the classic tropical Asian-American disjunct distribution of the genus *Perennihirschioporus*. This distribution could be the result of vicariance, where a once-continuous ancestral population was fragmented by continental drift (e.g., the breakup of Gondwana), or it could be the product of long-distance dispersal events. Compared to *Nigrohirschioporus, Perennihirschioporus* marks an initial evolutionary step towards adapting to seasonal climates, namely through its adaptation to seasonal drought. With a contribution of nearly 60% to the model, precipitation of the wettest quarter (Bio16) is the absolute master regulator of the genus's distribution. This indicates an extremely high degree of niche specialization. *Perennihirschioporus* is not merely a 'tropical' genus; it is a genus adapted specifically to tropical climates with a pronounced and intense wet season. This extreme dependence likely reflects a life cycle strategy that is tightly synchronized with seasonal monsoons. The massive influx of water during the wettest part of the year may be a critical trigger for breaking dormancy, facilitating rapid mycelial growth, and inducing the formation of its perennial basidiomata. In contrast, the ability to survive the pronounced dry season (as suggested by its presence in 'semi-arid' tropical climates) is a necessary secondary adaptation. This 'feast and famine' ecological strategy, tied to seasonal water availability, defines its highly restricted habitat. While precipitation is the primary driver, the importance of variables like isothermality (Bio3) and temperature seasonality (Bio4) highlights that this intense seasonal rainfall must occur within a stable thermal environment. The genus thrives where the temperature is consistently warm year-round, without the sharp fluctuations characteristic of temperate or high-altitude regions. This intolerance to temperature variability acts as another layer of filtering, preventing its colonization of otherwise suitably wet subtropical or montane areas. Its physiology appears to be finely tuned to the predictable warmth of the lowland tropics.

Unlike the strictly tropical genera, *Pallidohirschioporus* demonstrates remarkable ecological plasticity, representing a transitional evolutionary lineage that has successfully bridged tropical and temperate biomes. Our Maxent analysis suggests its distribution is governed not by annual averages, but by the interplay of seasonal extremes, and specifically, the availability of moisture during the dry season and sufficient warmth during the growing season. This points to a 'grow-and-survive' life history strategy: the genus capitalizes on warm, wet summers for rapid vegetative growth and fruiting, while possessing the physiological resilience to endure seasonal drought. However, this plasticity has limits. The sharp decline in habitat suitability where the mean temperature of the coldest quarter (Bio11) drops below freezing indicates a critical physiological barrier: intolerance to severe frost. This 'cold wall' effectively prevents *Pallidohirschioporus* from expanding into the high-latitude boreal forests dominated by *Hirschioporus*. Thus, ecologically, *Pallidohirschioporus* can be defined as a heat-adapted lineage that has expanded poleward as far as the frost line permits, occupying a broad niche distinct from both tropical specialists and boreal endemics.

In stark contrast, *Hirschioporus* represents a radical evolutionary niche shift from the ancestral tropical state of *Trichaptum* s.l. to a derived temperate-boreal specialization. This genus has evolved a strict dependency on cool, mesic environments, a trait that tightly correlates with its co-evolution with gymnosperm hosts (pines, spruces, firs) in the Northern Hemisphere. The most significant finding from our model is that the southern distribution limit of *Hirschioporus* is defined by a 'thermal ceiling' rather than a lack of resources. The high permutation importance of the maximum temperature of the warmest month (Bio5) reveals a fundamental physiological intolerance to summer heat. While saprotrophic fungi generally require moisture, *Hirschioporus* specifically requires moisture in conjunction with moderate temperatures to sustain its enzymatic activity. This thermal sensitivity effectively excludes the genus from lowland subtropical and tropical ecosystems, confining it to the 'climate islands' of high-altitude mountains or high-latitude boreal zones. Consequently, *Hirschioporus* exemplifies a trade-off in evolutionary adaptation: by specializing in cold-climate gymnosperm decomposition, it has lost the ancestral ability to tolerate the thermal stress of lower latitudes.

Family Trichaptaceae: the warm-temperate strategist

The family Trichaptaceae operates on a climatic principle that is fundamentally different from the adaptive radiation seen in the Hirschioporaceae. Its distribution is dictated not by seasonal averages, but instead by a hard physiological limit to extreme values. A key finding of our study is that the distribution of *Trichaptum* is governed by a dual thermal control mechanism. The minimum temperature of the coldest month (Bio6) acts as a hard physiological barrier, or a 'cold wall', preventing its northward and southward expansion into temperate zones. The sharp decline in habitat suitability below freezing temperatures (Supplementary Fig. S5b) indicates a fundamental intolerance to frost, a classic trait of tropical-subtropical lineages. This mechanism effectively defines the latitudinal limits of its range. Simultaneously, the high importance of the mean temperature of the warmest quarter (Bio10) reveals that the genus requires a 'heat engine' for its growth and reproduction. It doesn't just tolerate warmth; it thrives in it, with optimal conditions occurring in climates with hot summers (Supplementary Fig. S5d).

This requirement for high summer temperatures explains its concentration in lowland tropical and subtropical areas, distinguishing it from species that might tolerate cool summers. This dual dependence of avoidance of winter cold and affinity for summer heat paints a picture of a quintessential warm-climate specialist. While annual precipitation (Bio12) is undeniably crucial, as evidenced by its high contribution and the response curve showing a preference for very humid conditions (Supplementary Fig. S5c), its role appears to be that of a foundational requirement rather than a primary range-limiting factor at the global scale. The permutation importance analysis places thermal variables (especially Bio10) ahead of it. This implies that within the thermally suitable zones (i.e., areas that are not too cold in winter and are hot enough in summer) *Trichaptum* will then be filtered by moisture availability, preferentially occupying the wettest locations like rainforests. This hierarchical filtering, first by temperature, then by moisture, is a common pattern in niche structuring. This survival strategy, based on absolute extreme values rather than seasonal averages, is fundamentally different from the adaptive models of the four preceding genera.

Family Pseudotrichaptaceae: the extreme cold specialist

The monotypic family Pseudotrichaptaceae (genus *Pseudotrichaptum*) exhibits the most extreme specialization. In contrast to all other lineages, it is restricted to a highly specialized boreal-alpine specialist whose ecological niche is constrained by a strict 'two-way thermal filter'. A central finding of this study is that temperature acts as a 'two-way filter', setting both the southern and northern limits of the genus's range. The permutation importance analysis unequivocally identifies the maximum temperature of the warmest month (Bio5) as the most critical limiting factor. The sharp, cliff-like decline in habitat suitability above 20 °C (Supplementary Fig. S6c) acts as a 'heat barrier', effectively preventing *Pseudotrichaptum* from colonizing temperate regions with warmer summers. This intolerance to summer heat is a powerful physiological constraint that defines its southern boundary more strongly than any other factor. Conversely, while not the top-ranked variable, the response to annual mean temperature (Bio1), with a peak below freezing (Supplementary Fig. S6b), defines its core thermal environment. The genus is not just tolerant of cold; it is adapted to and likely requires a long, cold winter period for its life cycle, a common feature in boreal organisms. This adaptation to cold, combined with its intolerance to heat, creates a narrow thermal 'corridor' in which it can thrive. The significance of elevation as a predictor reinforces this, demonstrating that *Pseudotrichaptum* tracks these cold climates vertically into montane regions at lower latitudes. The seemingly paradoxical importance of precipitation of driest month (Bio14) is best understood as a proxy for these thermal conditions. In a circumboreal or alpine climate, the driest month is invariably the coldest winter month, where precipitation is locked away as snow and ice. The model's preference for low Bio14 values is therefore not an affinity for drought, but rather a reflection of the genus's profound adaptation to the arid conditions of a continental frozen winter.

The ecological strategy of *Pseudotrichaptum* is that of a quintessential boreal-alpine specialist. Its entire life history appears to be finely tuned to the rhythms of these cold, often harsh environments. It grows on a narrow range of hosts (conifers), is adapted to long periods of freezing temperatures, and is competitively excluded or physiologically constrained by the conditions of warmer climates. This high degree of specialization explains why, despite having spores that can travel long distances, its distribution remains strictly confined.

Conclusions

Overall, this study re-evaluated the species diversity and evolutionary origins of *Trichaptum* s.l. by collecting specimens from the Americas and Asia, using phylogenetical, morphological, molecular clock dating analyses, biogeographical data, morphological characteristics of basidiomata, as well as environmental factors, laying the foundation for future resource development and utilization.

Author contributions

The authors confirm contribution to the paper as follows: study conception and design: Zhou M, Yuan Y; data collection: Zhou M, Vlasák J; analysis and interpretation of results: Zhou M, Cui Y, Wu Y, Li C; draft manuscript preparation: Zhou M, Cui Y, Zeng G, Zhuang L. All authors reviewed the results and approved the final version of the manuscript.

Data availability

All data generated in the study are available in Table 2.

Acknowledgments

The research is supported by the National Natural Science Foundation of China (Project Nos 32400006, U23A20142, 32300013, 32370013), grants from Hainan Province Science and Technology Special Fund (ZDYF2023RDYL01), the Hainan Institute of National Park (HINP, KY-24ZK02), the Postdoctoral Fellowship Program (Grade C) of China Postdoctoral Science Foundation (GZC20230254) and the Young Elite Scientists Sponsorship Program by CAST (No. 2023QNRC001). We express our sincere gratitude to Heng Zhao (Institute of Applied Ecology, Chinese Academy of Sciences), Yucheng Dai (Beijing Forestry University), and Josef Vlasák Jr. (207 Silverbrook Dr., Schwenksville) for their generous provision of specimens and their strong support throughout this study.

Conflict of interest

All authors declare that they have no competing interests.

Supplementary information accompanies this paper online at: https://doi.org/10.48130/mycosphere-0026-0005.

Dates

Received 22 December 2025; Revised 29 January 2026; Accepted 3 February 2026; Published online 26 March 2026

References

[1] Wang K, Kirk PM, Yao YJ. 2020. Development trends in taxonomy, with special reference to fungi. *Journal of Systematics and Evolution* 58(4):406−412

[2] Bhunjun CS, Niskanen T, Suwannarach N, Wannathes N, Chen YJ, et al. 2022. The numbers of fungi: are the most speciose genera truly diverse? *Fungal Diversity* 114(1):387−462

[3] Wang F, Wang K, Cai L, Zhao M, Kirk PM, et al. 2023. Fungal names: A comprehensive nomenclatural repository and knowledge base for fungal taxonomy. *Nucleic Acids Research* 51:D708−D716

[4] Hibbett D, Nagy LG, Nilsson RH. 2025. Fungal diversity, evolution, and classification. *Current Biology* 35(11):R463−R469

[5] Hawksworth DL, Lücking R. 2017. Fungal diversity revisited: 2.2 to 3.8 million species. *Microbiology spectrum* 5(4):10

[6] Phukhamsakda C, Nilsson RH, Bhunjun CS, de Farias ARG, Sun YR, et al. 2022. The numbers of fungi: contributions from traditional taxonomic studies and challenges of metabarcoding. *Fungal Diversity* 114(1):327–386
[7] Hyde KD, Saleh A, Aumentado HDR, Boekhout T, Bera I, et al. 2024. Fungal numbers: Global needs for a realistic assessment. *Fungal Diversity* 128(1):191–225
[8] Hyde KD, Noorabadi MT, Thiyagaraja V, He MQ, Johnston PR, et al. 2024b. The 2024 Outline of fungi and fungus-like taxa. *Mycosphere* 15(1):5142–6239
[9] Al-Tanlimi S, Charleston M, Clayton D, Demastes J, Gray R. 2003. *Tangled trees: phylogeny, cospeciation, and coevolution*. Chicago and London: University of Chicago Press. 350 pp. www.researchgate.net/profile/Jean-Pierre-Hugot-2/publication/280881048
[10] Wiens JJ. 2004. Speciation and ecology revisited: phylogenetic niche conservatism and the origin of species. *Evolution* 58(1):193–197
[11] Seehausen O, Butlin RK, Keller I, Wagner CE, Boughman JW, et al. 2014. Genomics and the origin of species. *Nature Reviews Genetics* 15(3):176–192
[12] Taylor JW, Turner E, Townsend JP, Dettman JR, Jacobson D. 2006. Eukaryotic microbes, species recognition and the geographic limits of species: examples from the kingdom fungi. *Philosophical Transactions of the Royal Society B: Biological Sciences* 361(1475):1947–1963
[13] Schmit JP, Mueller GM. 2007. An estimate of the lower limit of global fungal diversity. *Biodiversity and Conservation* 16:99–111
[14] Taylor JW, Berbee ML. 2006. Dating divergences in the fungal tree of life: review and new analyses. *Mycologia* 98(6):838–849
[15] Vilgalys R, Sun BL. 1994. Assessment of species distributions in *Pleurotus* based on trapping of airborne basidiospores. *Mycologia* 86(2):270–274
[16] Hibbett DS. 2001. Shiitake mushrooms and molecular clocks: historical biogeography of *Lentinula*. *Journal of Biogeography* 28(2):231–241
[17] Varga T, Krizsán K, Földi C, Dima B, Sánchez-García M, et al. 2019. Megaphylogeny resolves global patterns of mushroom evolution. *Nature Ecology & Evolution* 3(4):668–678
[18] Zhao H, Nie Y, Zong TK, Wang K, Lv ML, et al. 2023. Species diversity, updated classification and divergence times of the phylum Mucoromycota. *Fungal Diversity* 123:49–157
[19] He MQ, Cao B, Liu F, Boekhout T, Denchev TT, et al. 2024. Phylogenomics, divergence times and notes of orders in Basidiomycota. *Fungal Diversity* 126(1):127–406
[20] Song HB, Bau T. 2024. Resolving the polyphyletic origins of *Pholiotina* s.l. (Bolbitiaceae, Agaricales) based on Chinese materials and reliable foreign sequences. *Mycosphere* 15(1):1595–1674
[21] Tremble K, Henkel T, Bradshaw A, Domnauer C, Brown LM, et al. 2024. A revised phylogeny of Boletaceae using whole genome sequences. *Mycologia* 116(3):392–408
[22] Dai YC, Wang Z, Binder M, Hibbett DS. 2006. Phylogeny and a new species of *Sparassis* (Polyporales, Basidiomycota): Evidence from mitochondrial atp6, nuclear rDNA and rpb2 genes. *Mycologia* 98:584–592
[23] Si J, Cui BK, He S, Dai YC. 2011. Optimization of conditions for laccase production by *Perenniporia subacida* and its application in dye decolorization. *Chinese Journal of Applied and Environmental Biology* 17(5):736–741
[24] Si J, Meng G, Wu Y, Ma HF, Cui BK, et al. 2019. Medium composition optimization, structural characterization, and antioxidant activity of exopolysaccharides from the medicinal mushroom *Ganoderma lingzhi*. *International Journal of Biological Macromolecules* 124:1186–1196
[25] Vainio EJ, Hakanpää J, Dai YC, Hansen E, Korhonen K, et al. 2011. Species of *Heterobasidion* host a diverse pool of partitiviruses with global distribution and horizontal transmission between species. *Fungal Biology* 115:1234–1243
[26] Wu F, Man X, Tohtirjap A, Dai Y. 2022. A comparison of polypore funga and species composition in forest ecosystems of China, North America, and Europe. *Forest Ecosystems* 9:100051
[27] Wu F, Zhou LW, Vlasák J, Dai YC. 2022c. Global diversity and systematics of *Hymenochaetaceae* with poroid hymenophore. *Fungal Diversity* 113:1–192
[28] Yuan Y, Bian LS, Wu YD, Chen JJ, Wu F, et al. 2023. Species diversity of pathogenic wood-rotting fungi (Agaricomycetes, Basidiomycota) in China. *Mycology* 14(3):204–226
[29] Ghobad-Nejhad M, Zhou LW, Tomšovský M, Angelini P, Cusumano G, et al. 2024. Unlocking nature's pharmacy: Diversity of medicinal properties and mycochemicals in the family Hymenochaetaceae (Agaricomycetes, Basidiomycota). *Mycosphere* 15(1):6347–6438
[30] Zhao H, Yuan HS, Cui YJ, Wang K, Wu F, et al. 2026. Global polypore diversity and distribution patterns. *Fungal Diversity* 136:136002
[31] Liu ZB, Yuan Y, Dai YC, Liu HG, Vlasák J, et al. 2025. Global diversity and systematics of Hymenochaetaceae with non-poroid hymenophore. *Fungal Diversity* 131:1–97
[32] Chen JJ, Cui BK, Zhou LW, Korhonen K, Dai YC. 2015. Phylogeny, divergence time estimation, and biogeography of the genus *Heterobasidion* (Basidiomycota, Russulales). *Fungal Diversity* 71(1):185–200
[33] Zhao H, Zhou M, Liu XY, Wu F, Dai YC. 2022. Phylogeny, divergence time estimation and biogeography of the genus *Onnia* (Basidiomycota, Hymenochaetaceae). *Frontiers in Microbiology* 13:907961
[34] Spirin V, Runnel K, Vlasák J, Viner I, Barrett MD, et al. 2024. The genus *Fomitopsis* (Polyporales, Basidiomycota) reconsidered. *Studies in Mycology* 107(1):149–249
[35] Zhao H, Wu F, Maurice S, Pavlov IN, Krutovsky KV, et al. 2025. Large-scale phylogenomic insights into the evolution of the Hymenochaetales. *Mycology* 16(2):617–634
[36] Vlasák J. 2017. *Trichaptum* (Basidiomycota) in tropical America: a sequence study. *Mycosphere* 8(1):1217–1227
[37] Kossmann T, Costa-Rezende DH, Góes-Neto A, Drechsler-Santos ER. 2021. A new and threatened species of *Trichaptum* (Basidiomycota, Hymenochaetales) from urban mangroves of Santa Catarina Island, Southern Brazil. *Phytotaxa* 482(2):197–207
[38] Mukhin VA, Knudsen H, Corfixen P, Zhuykova EV, Nepryakhin IO, et al. 2023. The genus *Trichaptum* in North Asia. *Mycology and Phytopathology* 57(4):255–266
[39] Zhou M, Dai YC, Vlasák J, Liu HG, Yuan Y. 2023. Revision and updated systematics of *Trichaptum* s.l. (Hymenochaetales, Basidiomycota). *Mycosphere* 14(1):815–917
[40] Saha R, Dutta AK, Acharya K. 2024. *Nigrohirschioporus violacaeruleum* sp. nov. and a new record of *Pallidohirschioporus brastagii* (Basidiomycota, Hymenochaetales) from India. *Phytotaxa* 634(2):131–142
[41] Murrill WA. 1904. The Polyporaceae of North America: IX. Inonotus, Sesia and monotypic genera. *Bulletin of the Torrey Botanical Club* 31(11):593–610
[42] Ryvarden L, Gilbertson RL. 1994. European polypores 2. Norway: Fungiflora, Oslo. pp. 394–743
[43] Núñez M, Ryvarden L. 2001. East Asian polypores 2. Polyporaceae s. lato. *Synop Fungorum* 14:170–522
[44] Dawson SK, Berglund H, Ovaskainen O, Jonsson BG, Snäll T, et al. 2024. Fungal trait-environment relationships in wood-inhabiting communities of boreal forest patches. *Functional Ecology* 38(9):1944–1958
[45] Zhang Y, Peng Z, Song Z, Schilling JS. 2025. Repeated measures of decaying wood reveal the success and influence of fungal wood endophytes. *mSystems* 10(9):e00382-25
[46] Yang XY, Feng T, Wang GQ, Ding JH, Li ZH, et al. 2014. Chemical constituents from cultures of the basidiomycete *Trichaptum pargamenum*. *Phytochemistry* 104:89–94
[47] Payamnoor V, Kavosi MR, Nazari J. 2020. Polypore fungi of *Caucasian alder* as a source of antioxidant and antitumor agents. *Journal of Forestry Research* 31:1381–1390
[48] Wang Y, Hausner G, Rout PR, Yuan Q. 2025. Investigation of fungal mycelium-bound bio-foams from agricultural wastes as sustainable and eco-conscious packaging innovations. *Journal of Cleaner Production* 501:145206
[49] Ganeshaiah K, Barve N, Chandrachekara K, Swamy M, Uma Shaanker R. 2003. Predicting the potrntial geographical distribution of the sugarcane wooly aphid using GARP and DIVA-GIS. *Current Science* 85(11):1526–1528
[50] Elith J, Graham CH, Anderson RP, Dudík M, Ferrier S, et al. 2006. Novel methods improve prediction of species' distributions from occurrence data. *Ecography* 29(2):129–151

[51] Peterson AT, Papeş M, Eaton M. 2007. Transferability and model evaluation in ecological niche modeling: a comparison of GARP and Maxent. *Ecography* 30(4):550–560

[52] Graham CH, Moritz C, Williams SE. 2006. Habitat history improves prediction of biodiversity in rainforest fauna. *Proceedings of the National Academy of Sciences of the United States of America* 103(3):632–636

[53] Kumar S, Stohlgren TJ. 2009. Maxent modeling for predicting suitable habitat for threatened and endangered tree *Canacomyrica monticola* in New Caledonia. *Journal of Ecology and natural Environment* 1(4):94–98

[54] Adhikari D, Barik SK, Upadhaya K. 2012. Habitat distribution modelling for reintroduction of Ilex khasiana Purk., a critically endangered tree species of northeastern India. *Ecological Engineering* 40:37–43

[55] Hernandez PA, Graham CH, Master LL, Albert DL. 2006. The effect of sample size and species characteristics on performance of different species distribution modeling methods. *Ecography* 29(5):773–785

[56] Ortega-Huerta MA, Townsend Peterson A. 2008. Modeling ecological niches and predicting geographic distributions: a test of six presence-only methods. *Revista mexicana de Biodiversidad* 79(1):205–216

[57] Young N, Carter L, Evangelista P. 2011. A MaxEnt model v3.3. e tutorial (ArcGIS v10). Natural Resource Ecology Laboratory, Colorado State University and the National Institute of Invasive Species Science. www.coloradoview.org/wp-content/coloradoviewData/trainingData/a-maxent-model-v8.pdf

[58] Yuan HS, Wei YL, Wang XG. 2015. Maxent modeling for predicting the potential distribution of *Sanghuang*, an important group of medicinal fungi in China. *Fungal Ecology* 17:140–145

[59] Mathur M, Mathur P. 2023. Prediction of global distribution of *Ganoderma lucidum* (Leys.) Karsten: a machine learning maxent analysis for a commercially important plant fungus. *Indian Journal of Ecology* 50(2):289–305

[60] Zhang QY, Liu HG, Papp V, Zhou M, Dai YC, et al. 2023. New insights into the classification and evolution of *Favolaschia* (Agaricales, Basidiomycota) and its potential distribution, with descriptions of eight new species. *Mycosphere* 14(1):777–814

[61] Dai YC. 2010. Hymenochaetaceae (Basidiomycota) in China. *Fungal Diversity* 45(1):131–343

[62] Anonymous. 1969. Flora of British fungi. Colour identification chart. Her Majesty's Stationery Office, London. pp. 1–3

[63] Petersen JH. 1996. The Danish Mycological Society's colour-chart. Foreningen til Svampekundskabens Fremme, Greve. pp. 1–6

[64] White TJ, Bruns T, Lee S, Taylor J. 1990. Amplification and direct sequencing of fungal ribosomal RNA genes for phylogenetics. In *PCR protocols: a guide to methods and applications*. vol. 18. Amsterdam: Elsevier. pp. 315–322 doi: 10.1016/B978-0-12-372180-8.50042-1

[65] Vilgalys R, Hester M. 1990. Rapid genetic identification and mapping of enzymatically amplified ribosomal DNA from several *Cryptococcus* species. *Journal of Bacteriology* 172(8):4238–4246

[66] Rehner SA, Buckley E. 2005. A *Beauveria* phylogeny inferred from nuclear ITS and EF1-α sequences: evidence for cryptic diversification and links to *Cordyceps teleomorphs*. *Mycologia* 97(1):84–98

[67] Katoh K, Standley DM. 2013. MAFFT Multiple sequence alignment software version 7: improvements in performance and usability. *Molecular Biology and Evolution* 30(4):772–780

[68] Hall TA. 1999. BioEdit: A user-friendly biological sequence alignment editor and analysis program for Windows 95/98/NT. *Symposium proceeding: Nucleic Acids Symposium Series, Oxford*. vol. 41. pp. 95–98

[69] Darriba D, Posada D, Kozlov AM, Stamatakis A, Morel B, Flouri T. 2020. ModelTest-NG: A new and scalable tool for the selection of DNA and protein evolutionary models. *Molecular Biology and Evolution* 37(1):291–294

[70] Stamatakis A. 2014. RAxML version 8: a tool for phylogenetic analysis and post-analysis of large phylogenies. *Bioinformatics* 30:1312–1313

[71] Ronquist F, Teslenko M, van derMark P, Ayres DL, Darling A, et al. 2012. MrBayes 3.2: efficient bayesian phylogenetic inference and model choice across a large model space. *Systematic Biology* 61(3):539–542

[72] Bouckaert R, Heled J, Kühnert D, Vaughan T, Wu CH, et al. 2014. BEAST 2: a software platform for Bayesian evolutionary analysis. *PLoS Computational Biology* 10(4):e1003537

[73] Hibbett DS, Grimaldi D, Donoghue MJ. 1995. Cretaceous mushrooms in amber. *Nature* 377(6549):487–487

[74] Hibbett D, Grimaldi D, Donoghue M. 1997. Fossil mushrooms from Miocene and Cretaceous ambers and the evolution of Homobasidiomycetes. *American Journal of Botany* 84(7):981–991

[75] Smith SY, Currah RS, Stockey RA. 2004. Cretaceous and Eocene poroid hymenophores from Vancouver Island, British Columbia. *Mycologia* 96(1):180–186

[76] Berbee ML, Taylor JW. 2010. Dating the molecular clock in fungi – how close are we? *Fungal Biology Reviews* 24(1):1–16

[77] Taylor TN, Hass H, Kerp H. 1999. The oldest fossil ascomycetes. *Nature* 399(6737):648–648

[78] Taylor TN, Hass H, Kerp H, Krings M, Hanlin RT. 2005. Perithecial ascomycetes from the 400 million year old Rhynie chert: an example of ancestral polymorphism. *Mycologia* 97(1):269–285

[79] Yu Y, Blair C, He X. 2020. RASP 4: ancestral state reconstruction tool for multiple genes and characters. *Molecular Biology and Evolution* 37(2):604–606

[80] Yu Y, Harris AJ, Blair C, He X. 2015. RASP (Reconstruct Ancestral State in Phylogenies): a tool for historical biogeography. *Molecular Phylogenetics and Evolution* 87:46–49

[81] Ryvarden L, Johansen I. 1980. *A preliminary polypore flora of East Africa*. Norway: Fungiflora, Oslo. 636 pp

[82] Ryvarden L. 1981. Type studies in the Polyporaceae. 13. Species described by JH Leveille. *Mycotaxon* 13:175–186

[83] Corner EJH. 1987. Ad Polyporaceas IV. The genera *Daedalea*, *Flabellophora*, *Flavodon*, *Gloeophyllum*, *Heteroporus*, *Irpex*, *Lenzites*, *Microporellus*, *Nigrofomes*, *Nigroporus*, *Oxyporus*, *Paratrichaptum*, *Rigidoporus*, *Scenidium*, *Trichaptum*, *Vanderbylia*, and *Steccherinum*. *Beih Nova Hedwigia* 86:1–265

[84] Dai YC. 2000. A checklist of polypores from Northeast China. *Karstenia* 40(1-2):23–29

[85] Hattori T. 2001a. Type studies of the polypores described by E.J.H. Corner from Asia and West Pacific areas II. Species described in *Gloeophyllum*, *Heteroporus*, *Microporellus*, *Oxyporus*, *Paratrichaptum*, and *Rigidoporus*. *Mycoscience* 42(1):19–28

[86] Hattori T. 2001b. Type studies of the polypores described by EJH Corner from Asia and West Pacific Areas III. Species described in *Trichaptum, Albatrellus, Boletopsis, Diacanthodes, Elmerina, Fomitopsis* and *Gloeoporus*. *Mycoscience* 42:423–431

[87] Ryvarden L, Iturriaga T. 2003. Studies in neotropical polypores 10. *New polypores from Venezuela. Mycologia* 95(6):1066–1077

[88] He MQ, Zhao RL, Hyde KD, Begerow D, Kemler M, et al. 2019. Notes, outline and divergence times of Basidiomycota. *Fungal Diversity* 99(1):105–367

[89] Wu G, Wu K, Halling RE, Horak E, Xu J, et al. 2023. The rapid diversification of Boletales is linked to Early Eocene and Mid-Miocene Climatic Optima. *bioRxiv* 563795

[90] Hay WW, Floegel S. 2012. New thoughts about the Cretaceous climate and oceans. *Earth-Science Reviews* 115(4):262–272

[91] Crisp MD, Cook LG. 2011. Cenozoic extinctions account for the low diversity of extant gymnosperms compared with angiosperms. *New Phytologist* 192(4):997–1009

[92] Jokat W, Boebel T, König M, Meyer U. 2003. Timing and geometry of early Gondwana breakup. *Journal of Geophysical Research: Solid Earth* 108:2002JB001802

[93] Hackel J, Henkel TW, Moreau PA, De Crop E, Verbeken A, et al. 2022. Biogeographic history of a large clade of ectomycorrhizal fungi, the Russulaceae, in the Neotropics and adjacent regions. *New Phytologist* 236(2):698–713

[94] Cui YJ, Wang CG, Dai YC, Liu S, Ren YH, et al. 2026. Phylogeny, divergence times, and biogeography of the phytopathogenic fungal genus *Phaeolus* (Basidiomycota, Polyporales). *Journal of Systematics and Evolution* 64(1):4–18

[95] Zhao H, Wu F, Dai YC, Vlasák J, Ghobad-Nejhad M, et al. 2025a. Divergence time and biogeography of the fungal genus *Porodaedalea*

(Basidiomycota, Hymenochaetales), obligate phytopathogens on coniferous trees. *Molecular Phylogenetics and Evolution* 212:108425
[96] Wang XW, May TW, Liu SL, Zhou LW. 2021. Towards a natural classification of *Hyphodontia* sensu lato and the trait evolution of basidiocarps within Hymenochaetales (Basidiomycota). *Journal of Fungi* 7(6):478
[97] Skrede I, Engh IB, Binder M, Carlsen T, Kauserud H, et al. 2011. Evolutionary history of Serpulaceae (Basidiomycota): molecular phylogeny, historical biogeography and evidence for a single transition of nutritional mode. *BMC Evolutionary Biology* 11:1–13
[98] Li J, Han LH, Liu XB, Zhao ZW, Yang ZL. 2020. The saprotrophic *Pleurotus ostreatus* species complex: late eocene origin in East Asia, multiple dispersal, and complex speciation. *IMA Fungus* 11(1):10
[99] Zhao H, Cui YJ, Guan QX, Wang K, Zhuang L, et al. 2025. Global fungal diversity and distribution patterns within the order Hymenochaetales (Agaricomycetes, Basidiomycota). *Mycosphere* 16(1):3257–3280
[100] Wu F, Fang X, Yang Y, Dupont-Nivet G, Nie J, et al. 2022a. Reorganization of Asian climate in relation to Tibetan Plateau uplift. *Nature Reviews Earth & Environment* 3(10):684–700
[101] Zachos J, Pagani M, Sloan L, Thomas E, Billups K. 2001. Trends, rhythms, and aberrations in global climate 65 Ma to present. *Science* 292(5517):686–693
[102] Donoghue MJ, Sanderson MJ. 2015. Confluence, synnovation, and depauperons in plant diversification. *New Phytologist* 207(2):260–274
[103] Sánchez-García M, Ryberg M, Khan FK, Varga T, Nagy LG, et al. 2020. Fruiting body form, not nutritional mode, is the major driver of diversification in mushroom-forming fungi. *Proceedings of the National Academy of Sciences* 117(51):32528–32534
[104] Bian LS, Wu F, Dai YC. 2016. Two new species of *Coltricia* (Hymenochaetaceae, Basidiomycota) from southern China based on evidence from morphology and DNA sequence data. *Mycological Progress* 15:27
[105] Wang W, Cawood PA, Pandit MK, Xia X, Raveggi M, et al. 2021. Fragmentation of South China from greater India during the Rodinia-Gondwana transition. *Geology* 49(2):228–232
[106] Zhou LW, Wang XW, Vlasák J, Ren GJ. 2018. Resolution of phylogenetic position of Nigrofomitaceae within Hymenochaetales (Basidiomycota) and *Nigrofomes sinomelanoporus* sp. nov. (Nigrofomitaceae) from China. *MycoKeys* 29:1–13
[107] Vu D, Groenewald M, de Vries M, Gehrmann T, Stielow B, et al. 2019. Large-scale generation and analysis of filamentous fungal DNA barcodes boosts coverage for kingdom fungi and reveals thresholds for fungal species and higher taxon delimitation. *Studies in Mycology* 92:135–154
[108] Jang Y, Jang S, Lee J, Lee H, Lim YW, et al. 2016. Diversity of wood-inhabiting polyporoid and *Corticioid* fungi in odaesan national park, Korea. *Mycobiology* 44(4):217–236
[109] Hoffmann K, Telle S, Walther G, Eckhart M, Kirchmair M, et al. 2008. Diversity, genotypic identification, ultrastructural and phylogenetic characterization of zygomycetes from different ecological habitats and climatic regions: limitations and utility of nuclear ribosomal DNA barcode markers. In *Current Advances in Molecular Mycology*, eds. Gherbawy Y, Mach RL, Rai M. Hauppauge: Nova Science Pub Inc. pp. 263–312
[110] Pitkäranta M, Meklin T, Hyvärinen A, Paulin L, Auvinen P, et al. 2008. Analysis of fungal flora in indoor dust by ribosomal DNA sequence analysis, quantitative PCR, and culture. *Applied and Environmental Microbiology* l74: 233–244
[111] Cho SE, Kwag YN, Jo JW, Han SK., Oh SH, et al. 2020. Macrofungal diversity of urbanized areas in southern part of Korea. *Journal of Asia-Pacific Biodiversity* 13(2):189–197
[112] Ko KS, Jung HS. 2002. Three nonorthologous ITS1 types are present in a polypore fungus *Trichaptum abietinum*. *Molecular Phylogenetics and Evolution* 23(2):112–122
[113] Ogura-Tsujita Y, Gebauer G, Xu H, Fukasawa Y, Umata H, et al. 2018. The giant mycoheterotrophic orchid *Erythrorchis altissima* is associated mainly with a divergent set of wood-decaying fungi. *Molecular Ecology* 27(5):1324–1337
[114] Papan S, Preedanon S, Saengkaewsuk S, Klaysuban A, Kobmoo N, et al. 2023. Genetic diversity of culturable fungi associated with scleractinian corals in the Gulf of Thailand. *Botanica Marina* 66(4):309–318
[115] Ko KS, Hong SG, Jung HS. 1997. Phylogenetic analysis of *Trichaptum* based on nuclear 18S, 5.8S and ITS ribosomal DNA sequences. *Mycologia* 89(5):727–734